

1 **Two Exopolyphosphatases with Distinct Molecular Architectures and Substrate**
2 **Specificities from the Thermophilic Green-sulfur Bacterium *Chlorobium tepidum* TLS**

3 *Tomás Albi & Aurelio Serrano*

4 Instituto de Bioquímica Vegetal y Fotosíntesis, Centro de Investigaciones Científicas Isla
5 Cartuja, CSIC-Universidad de Sevilla, Spain

6 *Corresponding author: Aurelio Serrano, Institute for Plant Biochemistry and Photosynthesis,
7 CSIC and University of Seville- 49th Americo Vespucio Avenue, 41092 Seville, Spain.
8 Telephone: +34 954 460 465; Fax: +34 954 460 165; E-mail: aurelio@ibvf.csic.es

9 **RUNNING TITTLE:** Two exopolyphosphatase homologs from *C. tepidum*

10 **KEYWORDS:** Exopolyphosphatase, tripolyphosphatase, Ppx-GppA phosphatase, NTPase,
11 short-chain polyphosphate, long-chain polyphosphate

12 **ABBREVIATIONS:** GP₄, guanosine 5'-tetraphosphate; Ni-NTA, nickel-nitrilotriacetic acid
13 metal-chelate; NTPase, nucleoside 5'-triphosphate γ -phosphate hydrolase; P₃, tripolyphosphate;
14 P_{3c}, trimetaphosphate (cyclic); P₁₃₋₁₈, polyphosphate mix (average chain length 13-18 phosphate
15 residues); polyP, inorganic polyphosphate; P_{LC}, long-chain polyP mix (>300 phosphate
16 residues); pNPP, *p*-nitrophenylphosphate; polyPase, Ppx-GppA polyphosphatase; PPK,
17 polyphosphate kinase; PPX, exopolyphosphatase

18 **DATABASE:** Nucleotide sequence data are available in the GenBank/EMBL/DDBJ databases
19 under the accession numbers HG764584.1 (*ppx1* construct), and HG764585.1 (*ppx2* construct).

20 Summary: 236 words.

21 Main text: 6485 words.

22 Tables: 1

23 Figures: 5

24 6 Supplementary Figures and 3 supplementary Tables are included

25 Contents Category. Physiology and Biochemistry.

26

27

28 **SUMMARY**

29 The genome of the thermophilic green-sulfur bacterium *Chlorobium tepidum* TLS possess two
30 genes encoding putative exopolyphosphatases (PPX, EC 3.6.1.11), namely CT0099 (*ppx1*, 993
31 bp) and CT1713 (*ppx2*, 1,557 bp). The predicted polypeptides of 330 and 518 amino acid
32 residues are Ppx-GppA phosphatases of different domain architectures - the largest one has an
33 extra C-terminal HD domain - which may represent ancient paralogs. Both *ppx* genes were
34 cloned and overexpressed in *Escherichia coli* BL21(DE3). While CtPPX1 was validated as a
35 monomeric enzyme, CtPPX2 was found to be a homodimer. Both PPX homologs were
36 functional, K⁺-stimulated phosphohydrolases with an absolute requirement for divalent metal
37 cations and a marked preference for Mg²⁺. Nevertheless, they exhibited remarkable different
38 catalytic specificities with regard to substrate classes and chain lengths. Even though both
39 enzymes were able to hydrolyze the medium-size polyphosphate P₁₃₋₁₈, CtPPX1 clearly reached
40 its highest catalytic efficiency with tripolyphosphate and showed substantial NTPase activity,
41 while CtPPX2 preferred long-chain polyphosphates (>300 Pi residues) and did not show any
42 detectable NTPase activity. These catalytic features, taken together with their distinct domain
43 architectures and molecular phylogenies, indicate that the two PPX homologs of *C. tepidum*
44 belong to different Ppx-GppA phosphatase subfamilies that should play specific biochemical
45 roles in nucleotide and polyphosphate metabolisms. Besides, these results provide an example
46 of the remarkable functional plasticity of the Ppx-GppA phosphatases, a family of proteins with
47 relatively simple structures which are widely distributed in the microbial world.

48

49 INTRODUCTION

50

51 Inorganic polyphosphates (polyP) are naturally occurring linear polymers of tens to hundreds of
52 orthophosphate residues linked by high-energy phosphoanhydride bonds. Despite being found
53 in every living being in nature – from bacteria to mammals (Kulaev *et al.*, 2005; Kornberg *et al.*,
54 1999) – and likely conserved from prebiotic times, the major attention to polyP has been its
55 role in heterotrophic, pathogenic bacteria (mainly gamma-proteobacteria and actinobacteria) and
56 yeasts. The PolyPs ubiquity suggests that they perform important roles in the cell that have been
57 changing during evolution. In prokaryotes, polyP has usually been described just as a polyanion
58 similar to ATP or other phosphate metabolites acting as a reservoir of energy (Kulaev *et al.*,
59 2005) or Pi (Urech *et al.*, 1978; Schuddemat *et al.*, 1989). Beyond that, polyPs have been
60 proved in a variety of ways to be essential for cell growth, responses to stresses and
61 stringencies, survival and for the virulence of pathogens (Ogawa *et al.*, 2000; Rashid &
62 Kornberg, 2000; Kim *et al.*, 2002; Shi *et al.*, 2004; Zhang *et al.*, 2005; Rao *et al.*, 2009; Nikel *et al.*,
63 2013).

64 PolyPs are synthesized in bacteria by polyP kinase (PPK; EC 2.7.4.1), which catalyzes the
65 readily reversible conversion of the terminal γ -phosphate of ATP to polyP (Rao *et al.*, 2009).
66 PolyP may be utilized as a substrate by transferases and hydrolases as well. They are degraded
67 to Pi by either endo- (PPN, EC 3.6.1.10) (Sethuraman *et al.*, 2001) or exopolyphosphatases
68 (PPX, EC 3.6.1.11). These later hydrolyse and processively release the terminal orthophosphate
69 from polyP which contains three or more phosphoanhydride bonds. Based on the primary
70 structure, two major non-homologous classes of PPX enzymes could be defined. Firstly, the
71 prototypic cytoplasmic ScPPX1 from yeast (ScPPX1) and its orthologs of fungi and protists,
72 which belong to the DHH-DHHA2 phosphoesterase family (Pfam, PF02833) that also includes
73 the well-characterized prokaryotic family II pyrophosphatases. ScPPX1 is an extremely active
74 phosphohydrolase with approximately 40 times the specific activity of the *E. coli*
75 polyphosphatase and it is able to efficiently hydrolyze polyP of 3 up to 1,000 Pi residues
76 (Lichko *et al.*, 2003). A second polyphosphatase class includes the Ppx-GppA phosphatases
77 (polyPases) (Pfam, PF02541) (Reizer *et al.*, 1993). They are widely distributed among bacteria
78 and archaea (Cardona *et al.*, 2002; Kristensen *et al.*, 2008), such as the polyPase PPX1 and
79 guanosine pentaphosphatase GPPA of *Escherichia coli*. The polyPase EcPPX1 of *E. coli*
80 is encoded by the *ppx1* gene which together the *ppk* gene form an operon (Akiyama *et al.*, 1992).
81 This polyPase processively and nearly completely hydrolyses the terminal residues of polyP to
82 Pi with a strong preference for long-chain substrates. EcPPX1 is a 58-kDa enzyme which forms
83 dimers in solution (Rangarajan *et al.*, 2006) and requires Mg^{2+} for maximal activity.
84 Alternatively, the second sequence-related *E. coli* exopolyphosphatase, designated as GPPA
85 (Keasling *et al.*, 1993), shows both polyPase and guanosine pentaphosphate phosphohydrolase
86 (GPPase, EC 3.6.1.40) activities. GPPase enzymes liberate Pi by processive hydrolysis of the
87 terminal phosphoanhydride bonds of long-chain polyP (1,000 residues) or by hydrolysis of
88 pppGpp to generate ppGpp, an intracellular alarmone or second messenger which controls the
89 bacterial stringent response, an adaptative process induced in response to nutrient starvation
90 (Rao *et al.*, 2009; Mechold *et al.*, 2013).

91 Hydrolysis of the shortest-polyP tripolyphosphate (P_3) has been reported in crude extracts of
92 bacteria, yeasts, protists and animal tissues. These ubiquitous tripolyphosphatase activities have
93 been usually associated with a range of proteins lacking sequence similarities with Ppx-GppA
94 polyPases, and described as promiscuous activities, towards substrates other than their natural
95 ones, of enzymes such as the inorganic pyrophosphatases (Jetten *et al.*, 1992; Baykov *et al.*,

96 1999; Kohn *et al.*, 2012), adenosylmethionine synthetase (Markham *et al.*, 1980; Perez Mato *et*
97 *al.*, 2001), DHH-DHHA2 exopolyphosphatases (Rodrigues *et al.*, 2002), the human metastasis
98 regulator protein H-Prune (Tammenkoski *et al.*, 2008) and the CYTH superfamily of tunnel
99 metalloenzymes which was named after its two founding members: the bacterial CyaB
100 adenylate cyclase and the mammalian thiamine triphosphatase (Bettendorff & Wins, 2013). A
101 group of CYTH proteins named triphosphate tunnel metalloenzymes (TTM) has been recently
102 found in some bacteria (eg. *Clostridium thermocellum*, *Nitrosomonas europaea*) (Keppetipola *et*
103 *al.*, 2007; Delvaux *et al.*, 2011) and the plant *Arabidopsis thaliana* (Moeder *et al.*, 2013), and
104 was reported to be highly specific inorganic tripolyphosphatases. However, the specific
105 metabolic roles of TTM proteins and its contribution, together with the more widespread Ppx-
106 GppA phosphatases, to the ubiquitous tripolyphosphatase activity have not been studied so far.

107 The presence of Ppx-GppA phosphatase paralogs has been reported so far only for the Gram-
108 positive actinobacteria *Corynebacterium glutamicum* ATCC 13032 (Lindner *et al.*, 2009) and
109 *Mycobacterium tuberculosis* H37Rv (Choi *et al.*, 2012). In both cases, two *ppx* genes encoding
110 putative polyPases with a single domain architecture (Ppx-GppA, Pfam PF02541) and similar
111 predicted molecular masses (ca. 35 kDa) were reported, but in neither case a full kinetic
112 characterization of the two paralogous proteins was carried out. Interestingly, a peculiar
113 scenario of two polyPase isoforms with some biochemical differences, probably generated by
114 proteolytic processing of a single PPX protein precursor, was reported for the actinobacterium
115 *Microlunatus phosphovorius* (Lichko *et al.*, 2002) for which has been thereafter shown to have a
116 single *ppx* gene (see below). Reported here will be the first, to our knowledge, comparative
117 study of two *ppx* paralogous genes of the anaerobic, phototrophic bacterium *Chlorobium*
118 *tepidum* that encode functional polyPases of different domain architectures. Its functional
119 characterization showed dramatic differences in substrate specificity against short- and long-
120 chain polyPs and nucleotides. The remarkable structural and catalytic differences found between
121 these bacterial PPX homologs strongly support them as members of two distinct subfamilies of
122 Ppx-GppA exopolyphosphatases with specific roles in nucleotides and phosphate metabolisms.

123

124 METHODS

125

126 **Reagents, strains and plasmids.** Linear sodium polyphosphates, PPI, P₃, P₁₃₋₁₈, and water-
127 insoluble Maddrell salt (crystalline long-chain polyphosphate of very high molecular mass),
128 cyclic trimetaphosphate P_{3c}, NTPs GP₄) were purchased from Sigma. When necessary, polyP
129 was washed twice with 3.5 ml of 70 % (v/v) ethanol, dried overnight in a vacuum dessicator,
130 and resuspended in 600 µl of distilled water. Very long chain polyPs with an average chain
131 length of approximately 800 phosphate residues (P_{LC}) were obtained by fractionation of
132 solubilized Maddrell salt, prepared as described by Becke-Goehring (1961), on a 2 % (w/v)
133 polyacrylamide/0.8 % (w/v) agarose gel. All other chemicals were of analytical grade.

134 The strain *Chlorobium tepidum* TLS-1 was kindly provided by Prof. Dr. Michael T.
135 Madigan (Southern Illinois University, Carbondale, IL, USA). *Escherichia coli* DH5a was used
136 as a host for cloning and propagation, and *E. coli* BL21 (DE3) was used for overexpression of
137 cloned genes. Plasmids pGEM®-T Easy and pQE-80L used as cloning and expression vectors,
138 respectively, were purchased from Promega and Qiagen.

139 **DNA manipulation.** Genomic DNA of *Chlorobium tepidum* (strain TLS-1/ATCC49652) was
140 extracted using the method described by Wahlund *et al.*, (1991). The PCR-amplified products
141 and plasmids were extracted with DNA gel extraction and Plasmid Miniprep kits from Sigma-
142 Aldrich (USA). *E. coli* competent cells preparation and transformation was performed according
143 to Green & Sambrook (2012).

144 **Cloning of two *C. tepidum* genes encoding putative Ppx-GppA phosphatases.** According
145 with the data published in the *Chlorobium tepidum* TLS genome (TIGR, 2002) (Eisen *et al.*,
146 2002), the complete ORFs for two paralogous genes encoding putative polyPases: *ppx1*
147 (gi_21645997) and *ppx2* (gi_21647723) were inferred. For expression in *E. coli*, these ORFs
148 were amplified by high-fidelity PCR using two pairs of specific primers, which for directional
149 cloning introduced up- and downstream restriction sites *Bam*HI and *Pst*I, respectively, as is
150 shown in Table S1. The PCR-amplified DNA fragments corresponding to the *ppx1* and *ppx2*
151 genes were recovered and cloned into pGEM®-T Easy vector for sequencing.

152 **Construction of recombinant plasmids and expression in *E. coli*.** The *ppx* genes were
153 digested with *Bam*HI and *Pst*I and then ligated into pQE-80L. In this way, a 6 His tag was
154 added to the N-terminal end of the native proteins. The recombinant plasmids were transformed
155 into *E. coli* BL21 (DE3), and the cells were incubated at 37 °C in 1 L Luria–Bertani (LB)
156 medium supplemented with 100 µg ml⁻¹ ampicillin with vigorous shaking. The cultures were
157 induced with 1 mM IPTG when the OD₆₀₀ of the culture increased to approximately 0.7 and
158 then incubated at 30 °C for 4 h with shaking at 200 rpm.

159 **Purification of the recombinant polyPases CtPPX1 and CtPPX2.** Cells were harvested
160 and resuspended in buffer A (200 mM NaCl, 5 mM MgCl₂, 10 mM imidazole, 25 mM Tris-HCl,
161 pH 8.0), then lysed by sonication at 4 °C. Cell debris was removed by centrifugation. The crude
162 extract was loaded onto a pre-equilibrated His-Trap HP 1 mL Ni-NTA column (GE-Healthcare).
163 Subsequently, non target proteins were removed by washing the column with buffer B (200 mM
164 NaCl, 5 mM MgCl₂, 50 mM imidazole, 25 mM Tris-HCl, pH 8.0) until no more protein elution
165 was observed. Finally, recombinant CtPPX1 and CtPPX2 were eluted by applying a linear
166 gradient with a target concentration of 100% of buffer C (200 mM NaCl, 5 mM MgCl₂, 500
167 mM imidazole, 25 mM Tris-HCl, pH 8.0) at a flow rate of 2 ml min⁻¹. Fractions containing the
168 purified proteins were pooled and dialyzed three times against with 50 mM Tris-HCl (pH 6.5)

169 buffer plus 5 mM MgCl₂ to remove imidazole and phosphate salts, then concentrated by
170 ultrafiltration (Amicon Ultra 3 kDa membranes), and eventually checked for polyPase activity.

171 **Analytical gel filtration chromatography.** Native molecular masses of CtPPX1 and CtPPX2
172 were determined using a FPLC gel filtration chromatography column (Superose 12 HR 10/30,
173 10×300 mm; GE-Healthcare, USA). Proteins were eluted with 200 mM NaCl, 5 mM MgCl₂, 50
174 mM Tris-HCl (pH 6.5) buffer at a flow rate of 2 ml min⁻¹. Native M_m values were calculated by
175 column calibration with six standard proteins of known molecular masses, including
176 thyroglobulin (Thy, 669 kDa), ferritin (Fer, 443 kDa), β-amylase (β-Amy, 200 kDa), alcohol
177 dehydrogenase (ADH, 150 kDa), carbonic anhydrase (CA, 29 kDa) and cytochrome c (Cyt.c,
178 12.4 kDa).

179 **Peptide mass fingerprinting and validation of CtPPX proteins by MALDI-TOF mass**
180 **spectrometry.** Protein samples corresponding to high-purity CtPPXs were derived from SDS-
181 PAGE. Proteins were digested with trypsin and the resulting peptides were extracted and loaded
182 onto a suitable MALDI matrix, and eventually processed by a MALDI-TOF mass spectrometer
183 (AutoFlex, Bruker-Daltonics, Proteomics Service of IBVF, CSIC-University of Seville) which
184 generated peptide mass spectra in the mass range 0.8–2.5 kDa. MASCOT-Matrix Science
185 database was used to analyze the peaks lists for protein identification (Koenig *et al.*, 2008).

186 **Exopolyphosphatase activity assays.** Unless otherwise stated, enzymatic activities were
187 measured using a standard assay mixture containing 50 mM Tris-HCl (pH 6.5) buffer, 5 mM
188 MgCl₂, 20 mM KCl, 1 mM P₁₃₋₁₈ (calculated as polyP, considering an average chain-length of
189 15 phosphate residues) and 10 μl of purified CtPPX at the adequate concentration, in a total
190 volume of 1 ml. Other polyPs, P_i, NTPs and GP₄ were used in the assays instead of P₁₃₋₁₈ when
191 the efficiencies of alternative substrates were tested. All reactions were performed at room
192 temperature (25 °C). NTPase, inorganic pyrophosphatase and polyPase activities were
193 determined by colorimetric measuring of released Pi with the ascorbic acid-ammonium
194 molybdate reagent (Ames, 1966; Gomez-Garcia, 2007). One Unit is defined as the amount of
195 enzyme catalyzing the release of 1 μmol of P_i per min under the standard conditions given.
196 Alkaline phosphatase activity was monitored spectrophotometrically at 405 nm by the cleavage
197 of pNPP (1 mM) at pH 7.5. Each enzymatic activity determination was carried out in triplicate
198 and mean values ± standard errors are provided.

199 **Determination of kinetic parameters.** The K_m of the purified enzymes were calculated using
200 mixtures containing concentrations of P₃, GP₄, or P₁₃₋₁₈ from 10 to 1,400 μM, at pH 6.5, and
201 0.6-1.1 μg of the indicated purified PPX in an assay volume of 1.0 ml. Kinetic parameters were
202 determined by nonlinear curve fitting from the Michaelis-Menten plot using the spreadsheet
203 Anemona.xlt (Hernandez & Ruiz, 1998).

204 **Effects of pH and metal cations on the activity of CtPPX proteins.** For the studies on the
205 effect of pH, CtPPX activities were measured in assay mixtures covering the pH range from 5.5
206 to pH 11.0 (increments of 0.5 pH units). The buffers used for optimal pH determinations were
207 MES (pH 5.5-7.0), MOPS (pH 7.0-8.0), Tris (pH 8.0-9.0), CHES (pH 9.0-10.0) and CHAPS
208 (10.0-11.0) at 50 mM final concentration, adjusted to the indicated pH ranges with NaOH or
209 HCl.

210 To investigate the effects of different divalent metal cations on the activity of CtPPX1
211 and CtPPX2, 5 mM of the corresponding chloride salts was added to the reaction mixture
212 instead of the Mg²⁺ salt. For this study, 8 mM EDTA was also included in the reaction mixture

213 to attest whether free-metal cofactor availability is a fundamental requirement for CtPPX
214 polyPase activity.

215

216 RESULTS AND DISCUSSION

217

218 Identification of *ppx* and *ppk* paralogous genes in the *C. tepidum* genome

219 The GenBank database was searched using the TBLASTN algorithm and the deduced
220 amino acid sequences of *E. coli ppk1* and *ppx* genes as queries (Akiyama *et al.*, 1992) to look for
221 homologs in the genomes of phototrophic bacteria. Several possible *ppx* and *ppk1* genes
222 encoding respectively polyPase and polyP kinase-like proteins, most of them annotated as
223 putative, were identified in the genomes of phylogenetically diverse phototrophic bacteria,
224 including anoxygenic photobacteria and cyanobacteria. Remarkably, pairs of *ppx* and *ppk1*
225 paralogous genes involved in polyP metabolism, likely generated by ancient gene duplications,
226 were found in the genome of the thermophilic green-sulfur bacterium *Chlorobium tepidum* TLS
227 (Eisen *et al.*, 2002). Subsequent analysis revealed that the two putative *ppx* genes – CT0099
228 (993 bp) and CT1713 (1,557 bp), hereafter referred as *ppx1* and *ppx2*, respectively – which are
229 located in different regions of the bacterial genome encode different Ppx-GppA phosphatase
230 proteins. Homologs of both genes were identified in cyanobacteria, other phototrophic bacteria
231 and a range of diverse heterotrophic prokaryotes (bacteria and archaea) (Gomez-Garcia *et al.*,
232 2003; Albi T and Serrano A, unpublished results). At the protein level, sequences analyses of
233 CtPPX1 (330 aa; nominal mass 35,799 Da) and CtPPX2 (518 aa; nominal mass 58,436 Da)
234 revealed a quite low level of amino acid identity to each other (ca. 27 % identity) on the
235 overlapping N-region (ca. 320 aa). This region encloses the Ppx-GppA domain (Pfam,
236 PF02541) containing a number of conserved motifs and conserved catalytic and
237 substrate/cofactor-binding residues involved in phosphatase activity, while the extra C-terminal
238 region exclusive of CtPPX2 (ca. 190 aa) harbour a HD domain (Pfam, PF01966) (Aravind &
239 Koonin, 1998) (Fig. S1). The identities shared between CtPPX1 and CtPPX2 with other
240 investigated Ppx-GppA proteins suggested distant evolutionary relationships between them:
241 while CtPPX1 shared higher identities (35-40 %) to one of the homologous proteins of *C.*
242 *glutamicum* and *M. tuberculosis*, CtPPX2 shared the highest identity (ca. 35 %) along its overall
243 sequence length to the polyPase of the cyanobacterium *Synechocystis* which also possess a C-
244 terminal HD domain (Table S2). In contrast, the two paralogous *ppk1* genes of *C. tepidum*,
245 CT0887 (*ppk1-1*; 2,097 bp) and CT 1049 (*ppk1-2*; 2,145 bp), encoded proteins which share a
246 remarkably high level of identity to each other, ca. 67 %, suggesting a relatively recent gene
247 duplication event in this case. Considering the high sequence homology between the two *C.*
248 *tepidum* PPKs, as well as with other previously studied PPK1 proteins (Rao *et al.*, 2009), we
249 decided to focus on the biochemical characterization of the two distinct PPX homologs with the
250 aim of providing insights of their specific biological roles.

251 Gene cloning and overproduction of recombinant CtPPX proteins

252 The putative *ppx* genes of *C. tepidum* were cloned from genomic DNA by PCR
253 amplification. DNA fragments with the expected size of 993 and 1,557 bp for *ppx1* and *ppx2*
254 genes respectively were obtained (Fig. 1a). They were initially cloned into pGEM-T Easy vector
255 and afterwards in the expression vector pQE-80L, so a six-His tag was eventually added to the
256 N-terminal in the recombinant proteins. The generated plasmids pTAR1/*Ctep* and pTAR2/*Ctep*
257 containing, respectively, the recombinant *ppx1* and *ppx2* genes were introduced into the
258 protease-deficient *E. coli* strain BL21. By the addition of IPTG, overexpression of *Chlorobium*
259 *ppx* genes induced in early-log phase cultures increased polyPase specific activity levels by
260 about 10-fold in the bacterial host. Cell extracts from induced *E. coli* cultures overproducing
261 CtPPX1 and CtPPX2 showed major protein bands of ca. 37 and 60 kDa on SDS-PAGE gels

262 (Fig. 1b) and high exopolyphosphatase specific activity levels with P_{13-18} as substrate, 0.4 and
263 $0.5 \mu\text{mol min}^{-1} \text{mg}^{-1}$, respectively. In contrast, extracts from cells containing the pQE-80L
264 plasmid with no insert did not show the aforementioned major protein bands on SDS-PAGE
265 gels and, furthermore, exhibited clearly lower specific activity levels, ca. $0.05 \mu\text{mol min}^{-1} \text{mg}^{-1}$,
266 probably due to the bacterial host PPX.

267 Milligram quantities of overproduced recombinant CtPPX1 and CtPPX2 were obtained
268 from the cell extracts (soluble protein fractions) after purification by Ni-NTA affinity
269 chromatography, following a standard procedure as described in Materials and Methods. Protein
270 elution profile showed in both cases a main peak overlapped with the single peak of polyPase
271 activity corresponding to the recombinant protein, which was eluted at an imidazole
272 concentration of 180 mM (Fig. S2). The purified recombinant proteins were then dialyzed to
273 remove imidazole and phosphate salts and concentrated by ultrafiltration. At this stage CtPPXs
274 were purified to 95-98% homogeneity as checked by SDS-PAGE analysis (data not shown).

275 **CtPPX1 and CtPPX2 have different native oligomeric states**

276 Ni-NTA chromatography purified CtPPX1 and CtPPX2 preparations were analyzed by
277 FPLC gel filtration chromatography on a Superose 12 HR column, which allowed a greater
278 purification level up to apparent electrophoretic homogeneity to be achieved (Fig. 1b). In both
279 cases, the elution profiles of protein and enzymatic activity showed single, symmetric
280 overlapped peaks, whose corresponding fractions exhibited on SDS-PAGE gels a single protein
281 band of ca. 37 and 59 kDa (Fig. 2). Native M_m values of 38.8 kDa for CtPPX1 and 100.4 kDa
282 for CtPPX2 were calculated. Therefore, CtPPX1 was validated as a catalytically active
283 monomeric enzyme, which is a rather unusual scenario for Ppx-GppA phosphatases, while
284 CtPPX2 is a homodimeric enzyme, with peak exopolyphosphatase activities in their FPLC
285 elution profiles of ca. 35 and $60 \mu\text{mol min}^{-1} \text{ml}^{-1}$, respectively. The only functional monomeric
286 polyPase reported so far is the PPX2 of *C. glutamicum* (Lindner *et al.*, 2009). Other bacterial
287 and archaeal Ppx-GppA phosphatases studied to date are functional homodimeric enzymes of
288 100-120 kDa (e.g. GPPase and PPX of *E. coli*) (Keasling *et al.*, 1993; Akiyama *et al.*, 1993).

289 At this final stage of the purification procedure, both CtPPXs were obtained as
290 functional, highly purified enzymes with a single polypeptide of 37.2 (CtPPX1) and 59.9
291 (CtPPX2) kDa on SDS-PAGE gels (Fig. 1b). The observed molecular masses are slightly higher
292 than those predicted from mRNAs, as expected for polyhistidine-tagged recombinant proteins.
293 Besides, the identities of the CtPPX1 and CtPPX2 polypeptides were confirmed by peptide
294 mass fingerprinting covering ca. 50-60% of the natural sequences, and eventual identification by
295 MALDI-TOF mass spectrometry (Fig. S3). As both isolated proteins were obtained as active
296 and highly pure preparations they were used for the kinetic characterization of the functional
297 polyPases from *C. tepidum*.

298 **Kinetic analyses reveal different catalytic features of CtPPX1 and CtPPX2**

299 *Preference for polyP of different chain lengths.* The substrate specificities and kinetic
300 parameters of recombinant CtPPX1 and CtPPX2 proteins were investigated, using polyPs of
301 different chain lengths and other phosphorylated substrates. Noteworthy, the CtPPXs
302 hydrolyzed linear polyP of very diverse chain lengths, from the simplest P_3 to P_{LC} of several
303 hundred (>300) Pi residues, but with clearly different catalytic preferences (Fig. 3a). The
304 highest specific activity for CtPPX1 was reached with P_3 (ca. $590 \pm 40 \mu\text{mol min}^{-1} \text{mg}^{-1}$) and
305 progressively dropped with longer polyPs to ca. 170 ± 4 and $15 \pm 1 \mu\text{mol min}^{-1} \text{mg}^{-1}$ with P_{13-18}

306 and P_{LC}, respectively. The opposite pattern was found for CtPPX2 which has a residual activity
307 with P₃ (ca. $6 \pm 0.5 \mu\text{mol min}^{-1} \text{mg}^{-1}$) and high phosphatase activities with longer polyPs such as
308 P₁₃₋₁₈ ($180 \pm 5 \mu\text{mol min}^{-1} \text{mg}^{-1}$) or P_{LC} ($126 \pm 4 \mu\text{mol min}^{-1} \text{mg}^{-1}$). No phosphatase activity was
309 observed with either CtPPX when using pNPP, PPi or the cyclic polyP trimetaphosphate (P_{3c}) as
310 substrates (see Fig. 3a). The K_m , V_{max} and k_{cat} values of CtPPXs were calculated for each of the
311 polyP substrates P₃, P₁₃₋₁₈ and guanosine tetrapolyphosphate GP₄ (summarized in Table 1). The
312 corresponding values could not be estimated for P_{LC} because it consists of a mixture of very
313 long polyPs (average value of 800 Pi residues) with quite different chain lengths. The turnover
314 number (k_{cat}) and catalytic efficiency (k_{cat} / K_m) values of CtPPX1 with P₃ as substrate were ca.
315 30 and 65-fold higher than those of CtPPX2. On the other hand, the same kinetic parameters of
316 CtPPX1 for a medium-chain polyP as P₁₃₋₁₈ were ca. 3 and 7-fold lower than those of CtPPX2
317 (Figs. S4 and S5). Overall, these data indicated that CtPPX homologs specifically hydrolyze
318 polyP of different chain lengths. CtPPX1 virtually operates as an inorganic tripolyphosphatase
319 while CtPPX2 clearly prefers very long chain polyPs. At this respect, it is interesting to note
320 that bacterial and plant TTM proteins, which are structurally different from polyPases, have
321 been found to be very active and specific tripolyphosphatases (Moeder *et al.*, 2013). This raises
322 a possible scenario of unrelated protein families playing apparently redundant biochemical
323 functions in certain organisms.

324 *CtPPX1 has nucleoside triphosphatase activity.* Once stated that purified CtPPX1 has a
325 strong preference for short-chain polyPs as P₃, it was tested whether this recombinant polyPase
326 also possess nucleoside triphosphatase (NTPase) activity (EC 3.6.1.15). Previous studies
327 reported that *E. coli* PPX (Akiyama *et al.*, 1993), *C. glutamicum* PPX2 (Lindner *et al.*, 2009),
328 and *M. tuberculosis* MTB-PPX1 (Choi *et al.*, 2012) possess modest ATPase activities.
329 Noteworthy, CtPPX1 was found to hydrolyze ATP and UTP ($70\text{-}95 \mu\text{mol min}^{-1} \text{mg}^{-1}$) at similar
330 levels that the polyP P₁₃₋₁₈ usually used in the polyPase assays, and to a lesser degree GTP, CTP
331 and TTP ($20\text{-}30 \mu\text{mol min}^{-1} \text{mg}^{-1}$) (Fig. 3b), but not phosphorylated carbon metabolites (glucose
332 6-P, fructose, fructose 6-P, fructose 1,6-dP). Noteworthy, when the organic tetrapolyphosphate
333 GP₄ was used as a substrate for CtPPX1 higher levels of phosphatase activity (ca. 430 ± 20
334 $\mu\text{mol min}^{-1} \text{mg}^{-1}$), similar to those determined for P₃, were achieved (Fig. 3b). This suggested
335 that the nucleoside part of the NTPs cause hindrance of catalysis on the terminal phosphate
336 residue. In contrast, CtPPX2 showed no detectable phosphatase activity with any NTP, and only
337 a residual activity was observed with GP₄ (ca. $5 \mu\text{mol min}^{-1} \text{mg}^{-1}$) (Fig. 3b). Kinetic parameters
338 clearly showed that CtPPX1 was much more active and efficient than CtPPX2 with GP₄, ca. 30-
339 fold (Table 1, Figs. S4 and S5). It remains to be seen whether the bacterial alarmones pppGpp
340 and ppGpp, no commercially available so far, are substrates and/or inhibitors on the polyPase or
341 NTPase activities of CtPPX proteins. It cannot be excluded, therefore, that ppGpp may produce
342 an inhibitory effect on these polyPases, as was previously reported for the *M. tuberculosis* and
343 *E. coli* PPXs (Choi *et al.*, 2012; Kuroda *et al.*, 1997). At this respect, it is interesting to note that
344 GTP and to a lesser degree PPi were inhibitors of CtPPX1 tripolyphosphatase activity (K_i values
345 of 0.4 and 3.8 mM, respectively) while others NTPs were not. In contrast, none of NTPs tested
346 significantly inhibited CtPPX2 activity with P₁₃₋₁₈ as a substrate.

347 *Requirements for mono and divalent metal cations.* CtPPX1 and CtPPX2 did not require
348 K⁺ for their enzymatic activities, but like most previously characterized bacterial polyPases
349 (Lindner *et al.*, 2009; Choi *et al.*, 2013; Lichko *et al.*, 2002; Akiyama *et al.*, 1993; Bonting *et*
350 *al.*, 1993) they were clearly stimulated (about 3-fold) by the addition of 20 mM KCl (data not
351 shown). In contrast, the phosphohydrolase activity of both polyPases was absolutely dependent

352 on the presence of divalent metal cations in the reaction mixture. Maximum activity was
353 reached with 5 mM Mg^{2+} , and was dramatically reduced (down to 10%) by an excess of the
354 chelating agent EDTA (Fig. 3c). This result agrees with the fact that most polyPases of
355 microorganisms are stimulated by divalent metal cations (Rao *et al.*, 2009). The requirement for
356 a divalent metal cofactor can be partially accomplished to different extents by a number of
357 divalent cations, Mn^{2+} , Co^{2+} and Fe^{2+} being the most effective among all tested (Fig. 3c). For
358 instance, the reaction rates with 5 mM Mn^{2+} were approximately 37 % and 65 % of that
359 obtained with Mg^{2+} for CtPPX1 and CtPPX2, respectively (Fig. 3c). However, no additive
360 effects were observed, since in the presence of 5 mM Mn^{2+} an equal concentration of Mg^{2+} did
361 not activate CtPPXs further.

362 *Different pH activity profiles.* Although polyPase activities of CtPPX1 and CtPPX2
363 have similar slightly acidic pH optima (ca. 6.5) they exhibit remarkable differences in their pH
364 dependence profiles (Fig. 4). CtPPX1 activity with P_3 as a substrate showed a markedly steeper
365 pH curve that dropped down to 30-40% of the maximum level at both acid and alkaline sides of
366 the fairly narrow activity peak (pH range 5.5-7.5), with a quite modest activity remaining at pH
367 values higher than 9.5 (Fig. 4). A similar pH profile was found when CtPPX1 activity was
368 assayed with P_{13-18} as a substrate. In contrast, CtPPX2 activity with P_{LC} as a substrate showed a
369 pH profile with a broad plateau along the alkaline pH range, so most polyPase activity, nearly
370 90 % of the maximum value, remained at pH 10 (Fig. 4).

371 **CtPPX1 and CtPPX2 belong to different subfamilies of Ppx-GppA phosphatases**

372 The catalytic and structural differences found between the two polyPase homologs of *C.*
373 *tepidum* prompted us to carry out a molecular phylogenetic study to clarify their evolutionary
374 relationships with other members of the Ppx-GppA protein superfamily. Proteins containing the
375 Ppx-GppA domain are members of the sugar kinase/actin/hsp-70 superfamily and are different
376 in both sequence and structure from the functionally related RelA/SpoT enzymes that modulate
377 the stringent response via synthesis and degradation of (p)ppGpp (Cashel *et al.*, 1996). Ppx-
378 GppA proteins are ubiquitous among bacteria and archaea, and typically perform enzymatic
379 roles as polyPases and/or GPPases (Reizer *et al.*, 1993). In contrast, the only group of Ppx-
380 GppA proteins reported so far in eukaryotes - the so-called RTG2 proteins of fungi - are
381 regulatory proteins with hitherto unknown polyPase/GPPase activities that may function as
382 protein phosphatases (Jazwinski 2005); they are involved in the retrograde response, an adaptive
383 signalling pathway of altered mitochondria to the cell nucleus (Liao & Butow, 1993).

384 To analyze the molecular phylogenetic relationships of the two CtPPX homologs with
385 other bacterial, archaeal and eukaryotic Ppx-GppA proteins, a molecular phylogenetic tree was
386 constructed using sequences from selected species representatives of the main bacterial/archaeal
387 groups and the eukaryotic RTG2 proteins, with special emphasis on potential paralogy scenarios
388 among Ppx-GppA proteins (Fig. 5, Table S3). A number of relevant issues came out from this
389 analysis. Six major assemblies of Ppx-GppA proteins with diverse domain architectures and
390 phylogenetic distributions are defined. CtPPX1 and CtPPX2 arrange with all other Chlorobian
391 orthologs in separated compact clusters included respectively into two major evolutionary-
392 distant Ppx-GppA phosphatases subfamilies: the single-domain polyPases of low- M_m (35-40
393 kDa), with dual tripolyphosphatase-NTPase activity, and the larger two-domain Ppx-GppA -
394 HD polyPases (ca. 60 kDa), which displayed a strong preference for long-chain polyP (Fig. 5).
395 The first polyPase class presents a broad distribution among major bacterial clades
396 (Bacteroidetes/Chlorobia, Actinobacteria, α - and δ -Proteobacteria, Clostridia, Sinergistetes and

397 Nitrospirae); however, the latter class is prevailing among diverse phototrophic prokaryotes
398 (Chlorobia, Chloroflexi, Cyanobacteria, Heliobacteria), methanogenic Euryarchaea
399 (Methanomicrobiales), Bacilli, Spirochaetes, and other bacterial clades well adapted to
400 oligotrophic and/or extreme environments (e.g. the *Thermus/Deinococcus* group). It should be
401 noted at this point that the two previously studied CtPPX1-like Ppx-GppA paralogs from the
402 actinobacteria *C. glutamicum* and *M. tuberculosis* are highly active on P₃ and possess ATPase
403 activity (Lindner *et al.*, 2009; Choi *et al.*, 2012) but in neither case a full kinetic characterization
404 of their polyPase and NTPase activities was performed. On the other hand, although the
405 function of the HD domain still remains unknown, a possible role for CtPPX2 in adaptive
406 environmental responses, as was proposed for long-chain polyPs (Lindner *et al.*, 2009), can also
407 be envisaged as it was reported in a broad superfamily of HD-domain hydrolases involved
408 among other functions in the bacterial stringent response (Kuroda *et al.*, 1997). It should be
409 noted at this respect that the gene encoding the Ppx-GppA-HD polyPase ortholog of the
410 cyanobacterium *Synechocystis* sp. PCC6803 is a component of the Pho regulon strongly induced
411 by P deprivation, showing conspicuous oscillations of transcript levels driven by the daily cycle
412 (Gomez-Garcia *et al.*, 2003; Gomez-Garcia *et al.*, 2013).

413 Closely related to the HD-domain polyPases assembly and, like them, having a strong
414 preference for long-chain polyPs, emerge the GPPases and GPPase-like polyPases clades as two
415 sister groups of functionally different Ppx-GppA phosphatases paralogs, generated by ancient
416 duplication from a common ancestor (Fig. 5). They are large single-domain Ppx-GppA proteins
417 with a C-terminal extra region (55-60 kDa) highly active on long-chain polyPs and GPP, and
418 prevailing among γ - and β -proteobacteria (mostly enterobacteria) (Keasling *et al.*, 1993). The
419 remaining three major subfamilies of Ppx-GppA proteins conform a broad assembly including
420 1) a cluster of large polyPases (ca. 60 kDa) with a C-terminal region without specific domain
421 assignment found in α -proteobacteria only as paralogs of the CtPPX1-like small polyPases-
422 NTPases; 2) a second group of single-domain polyPases (35-45 kDa) highly active on long-
423 chain polyPs but with very low or residual NTPase/GPPase activities (Choi *et al.*, 2012), and
424 found in Actinobacteria, ϵ -proteobacteria, Bacilli, Rickettsia, some primitive bacterial groups
425 (Aquificae, Thermotogae) and Archaea; and 3) the cluster of eukaryotic RTG2 signalling
426 proteins of fungi and choanoflagellates (Liao & Butow, 1993) with no polyPase activity
427 reported so far. Interestingly, some peripheral basal sequences of bacterial endocellular
428 parasites/symbionts of eukaryotes (e.g. *Protochlamydia amoebophila*) appear also included in
429 the latter clade (Fig. 5, Table S3).

430 Pairs of polyPase paralogs seems to occur in evolutionary diverse bacterial groups. In
431 most cases, PPX paralogs belong to distinct Ppx-GppA subfamilies and exhibit different
432 structural properties, as we report in this study, suggesting ancient paralogy events. However, in
433 some cases closely related paralogs are found within the same Ppx-GppA subfamily suggesting
434 more recent gene duplications and possible functional diversification (see Fig. 5 and Table S3).
435 These findings support specific biochemical roles for these homologous proteins, mostly
436 associated to signalling pathways and/or environmentally regulated metabolic processes. In any
437 case, these recurrent evolutionary scenarios strongly suggest that Ppx-GppA proteins should
438 play important roles in adaptive cellular metabolism. It is interesting to note at this respect that
439 neither of the CtPPX paralogous genes seems to be organized in hypothetical polyP operons as
440 in the case for *E. coli* (Akiyama *et al.*, 1993), as was inferred from their genome localizations
441 (Fig. S6).

442 The notable structural and evolutionary diversities of Ppx-GppA proteins should
443 correlate with their remarkable functional plasticity, as this work has demonstrated. It should be
444 noted that the structurally simplest CtPPX1-like polyPases represent the only one Ppx-GppA
445 subfamily with paralogy relationships with several other distinct Ppx-GppA subfamilies
446 including polyPases highly active on long-chain polyPs (Fig. 5, Table S3). This, together with
447 the extreme simplicity of their preferred substrate – P_3 is the simplest polyP – strongly support
448 an ancient position within the Ppx-GppA superfamily. One can speculate with a possible
449 ancestral role of P_3 in the origin of life as a precursor of NTPs, similar to that proposed for PPI
450 in bioenergetics evolution (Serrano *et al.*, 2007). However, the current physiological role of P_3
451 remains obscure. It could play a role at the interface between nucleotide and polyphosphate
452 metabolisms as the catalytic properties of CtPPX1-like polyPases and other apparently
453 redundant but structurally distinct tripolyphosphatases (Lindner *et al.*, 2009) strongly suggest.
454 Nevertheless, P_3 has never been reported in prokaryotes in contrast to long-chain polyPs,
455 although it is known as an intermediate in a number of biosynthetic pathways, e.g. of S-
456 adenosylmethionine, and is generated in some enzymatic processes (Bettendorff & Wins, 2013;
457 Delvaux *et al.*, 2011). In contrast to this, P_3 has been shown as a major polyP in
458 acidocalcisomes of several parasitic protists (Moreno *et al.*, 2000), the vacuole of yeast (Castro
459 *et al.*, 1995) and the halotolerant microalga *Dunaliella* (Pick & Weiss 1991), and the
460 acidocalcisome-like, mitochondrial and nuclear compartments of mammalian cells (Kumble &
461 Kornberg, 1995; Abramov *et al.*, 2007; Muller *et al.*, 2009; Seidlmayer *et al.*, 2012). Moreover,
462 most of the few eukaryotic DHH-DHHA2 polyphosphatases studied so far exhibit high
463 tripolyphosphatase activity (Rodrigues *et al.*, 2002, Fang *et al.*, 2007, Tammenkoski *et al.*,
464 2008) and some of them, like the H-Prune protein, are involved in gene regulation and cell
465 proliferation (Tammenkoski *et al.*, 2008). Remarkably, a soluble DHH-DHHA2
466 exopolyphosphatase involved in cellular osmoregulation of the protist *Trypanosoma cruzi* is,
467 like CtPPX1, highly active with both P_3 and GP_4 , and has very low activity with long-chain
468 polyP (Fang *et al.*, 2007). Taking into account the known roles of prokaryotic GPPases and
469 eukaryotic RTG2 and Prune proteins in transcriptional gene activation, one can speculate on a
470 possible cellular regulatory function for P_3 and CtPPX1-like polyPases. In any case, it may be
471 expected that with the development of novel more sensitive methods it will be possible to
472 determine P_3 concentration and subcellular localization as an essential step towards the
473 understanding of their possible biological roles.

474

475 ACKNOWLEDGMENTS

476 The authors thank Prof. M. T. Madigan (Dept. of Microbiology, Southern Illinois
477 University, USA) for generously providing a sample of *Chlorobium tepidum* TLS cells. This
478 work was supported by research grants from the Spanish (BFU2004-00843, BFU2007-61887
479 and BFU2010-15622) and Andalusian Regional (PAIDI group BIO-261) Governments, all of
480 them partially funded by the EU FEDER program. PAIDI group BIO-261 belongs to the CeIA3
481 and AndalucíaTECH University Campuses of International Excellence. Authors thank Dr. M.-
482 R. Gómez-García for helpful suggestions and discussions.

483

484 REFERENCES

- 485 **Abramov, A. Y., Fraley, C., Diao, C. T., Winkfein, R., Colicos, M. A., Duchen, M. R.,**
486 **French, R. J. & Pavlov, E. (2007).** Targeted polyphosphatase expression alters mitochondrial
487 metabolism and inhibits calcium-dependent cell death. *Proc Natl Acad Sci U S A* **104**, 18091-
488 18096.
- 489 **Akiyama, M., Crooke, E. & Kornberg, A. (1992).** The polyphosphate kinase gene of
490 *Escherichia coli*. Isolation and sequence of the ppk gene and membrane location of the protein.
491 *J Biol Chem* **267**, 22556-22561.
- 492 **Akiyama, M., Crooke, E. & Kornberg, A. (1993).** An exopolyphosphatase of *Escherichia*
493 *coli*. The enzyme and its ppx gene in a polyphosphate operon. *J Biol Chem* **268**, 633-639.
- 494 **Ames, B. N. (1966).** Assay of inorganic phosphate, total phosphate and phosphatases. In
495 *Methods in Enzymology*, vol. Volume 8, pp. 115-118. Edited by V. G. Elizabeth F. Neufeld:
496 Academic Press.
- 497 **Aravind, L. & Koonin, E. V. (1998).** The HD domain defines a new superfamily of metal-
498 dependent phosphohydrolases. *Trends Biochem Sci* **23**, 469-472.
- 499 **Baykov, A. A., Cooperman, B. S., Goldman, A. & Lahti, R. (1999).** Cytoplasmic Inorganic
500 Pyrophosphatase. In *Inorganic Polyphosphates* (Progress in Molecular and Subcellular
501 Biology), vol. 23, pp. 127-150. Edited by H. Schröder & W. G. Müller: Springer Berlin
502 Heidelberg.
- 503 **Becke-Goehring, M. (1961).** Phosphorus and its Compounds, Bd. 1: Chemistry, von J. R. Van
504 Wazer. Interscience Publishers, New York-London 1958. *Angewandte Chemie* **73**, 552-552. doi:
505 10.1002/ange.19610731513.
- 506 **Benson, D. A., Cavanaugh, M., Clark, K., Karsch-Mizrachi, I., Lipman, D. J., Ostell, J. &**
507 **Sayers, E. W. (2013).** GenBank. *Nucleic Acids Res* **41**, D36-42.
- 508 **Bettendorff, L. & Wins, P. (2013).** Thiamine triphosphatase and the CYTH superfamily of
509 proteins. *FEBS J* **280**, 6443-6455.
- 510 **Bonting, C. F., Kortstee, G. J. & Zehnder, A. J. (1993).** Properties of polyphosphatase of
511 *Acinetobacter johnsonii* 210A. *Antonie Van Leeuwenhoek* **64**, 75-81.
- 512 **Cardona, S. T., Chavez, F. P. & Jerez, C. A. (2002).** The exopolyphosphatase gene from
513 *Sulfolobus olfataricus*: characterization of the first gene found to be involved in polyphosphate
514 metabolism in archaea. *Appl Environ Microbiol* **68**, 4812-4819.
- 515 **Cashel, M., Gentry, D., Hernandez, V. J. & Vinella, D. (1996).** The stringent response, 2nd
516 ed. In *Escherichia coli* and *Salmonella typhimurium*: cellular and molecular biology, p. 1458-
517 1496. Edited by F. C. Neidhardt *et al.* ASM Press, Washington, DC.
- 518 **Castro, C. D., Meehan A. J., Koretsky A. P. & Domach, M. M. (1995)** In situ ³¹P nuclear
519 magnetic resonance for observation of polyphosphate and catabolite responses of chemostat-
520 cultivated *Saccharomyces cerevisiae* after alkalisation. *Appl. Environ. Microbiol.* **61**, 4448-
521 4453.

522 **Choi, M. Y., Wang, Y., Wong, L. L., Lu, B. T., Chen, W. Y., Huang, J. D., Tanner, J. A. &**
523 **Watt, R. M. (2012).** The two PPX-GppA homologues from *Mycobacterium tuberculosis* have
524 distinct biochemical activities. *PLoS One* **7**, e42561.

525 **Delvaux, D., Murty, M. R., Gabelica, V., Lakaye, B., Lunin, V. V., Skarina, T.,**
526 **Onopriyenko, O., Kohn, G., Wins, P. & other authors (2011).** A specific inorganic
527 triphosphatase from *Nitrosomonas europaea*: structure and catalytic mechanism. *J Biol Chem*
528 **286**, 34023-34035.

529 **Eisen, J. A., Nelson, K. E., Paulsen, I. T., Heidelberg, J. F., Wu, M., Dodson, R. J., Deboy,**
530 **R., Gwinn, M. L., Nelson, W. C. & other authors (2002).** The complete genome sequence of
531 *Chlorobium tepidum* TLS, a photosynthetic, anaerobic, green-sulfur bacterium. *Proc Natl Acad*
532 *Sci U S A* **99**, 9509-9514.

533 **Fang, J., Ruiz F. A., Docampo M., Luo S., Rodrigues J. C. F., Motta L. S., Rohloff, P. &**
534 **Docampo R. (2007).** Overexpression of a Zn²⁺-sensitive soluble exopolyphosphatase from
535 *Trypanosoma cruzi* depletes polyphosphate and affects osmoregulation. *J Biol Chem* **282**,
536 32501-32510.

537 **Fujisawa, T., Okamoto, S., Katayama, T., Nakao, M., Yoshimura, H., Kajiya-Kanegae, H.,**
538 **Yamamoto, S., Yano, C., Yanaka, Y. & other authors (2014).** CyanoBase and RhizoBase:
539 databases of manually curated annotations for cyanobacterial and rhizobial genomes. *Nucleic*
540 *Acids Res* **42**, D666-670.

541 **Gomez-Garcia, M. R., Losada, M. & Serrano, A. (2003).** Concurrent transcriptional
542 activation of ppa and ppx genes by phosphate deprivation in the cyanobacterium *Synechocystis*
543 sp. strain PCC 6803. *Biochem Biophys Res Commun* **302**, 601-609.

544 **Gomez-Garcia, M. R., Losada, M. & Serrano, A. (2007).** Comparative biochemical and
545 functional studies of family I soluble inorganic pyrophosphatases from photosynthetic bacteria.
546 *FEBS J* **274**, 3948-3959.

547 **Gomez-Garcia, M. R., Fazeli, F., Grote, A., Grossman, A. R. & Bhaya, D. (2013).** Role of
548 polyphosphate in thermophilic *Synechococcus* sp. from microbial mats. *J Bacteriol* **195**, 3309-
549 3319.

550 **Gouy, M., Guindon, S. & Gascuel, O. (2010).** SeaView version 4: A multiplatform graphical
551 user interface for sequence alignment and phylogenetic tree building. *Mol Biol Evol* **27**, 221-
552 224.

553 **Green, M. R. & Sambrook, J. (2012).** *Molecular cloning: a laboratory manual*, 4th edn. Cold
554 Spring Harbor, NY: Cold Spring Harbor Laboratory.

555 **Hernandez, A. & Ruiz, M. T. (1998).** An EXCEL template for calculation of enzyme kinetic
556 parameters by non-linear regression. *Bioinformatics* **14**, 227-228.

557 **Igor S. Kulaev, V. V., Tatiana Kulakovskaya (2005).** The Biochemistry of Inorganic
558 Polyphosphates, 2nd edn.

559 **Igor S. Kulaev, V. V., Tatiana Kulakovskaya (2005).** *The Biochemistry of Inorganic*
560 *Polyphosphates*, 2nd edn. Chichester, UK. : John Wiley & Sons, Ltd.

561 **Jazwinski, S. M. (2005).** Rtg2 protein: at the nexus of yeast longevity and aging. *FEMS Yeast*
562 *Res* **5**, 1253-1259.

563 **Jetten, M. S., Fluit, T. J., Stams, A. J. & Zehnder, A. J. (1992).** A fluoride-insensitive
564 inorganic pyrophosphatase isolated from *Methanothrix soehngenii*. *Arch Microbiol* **157**, 284-
565 289.

566 **Keasling, J. D., Bertsch, L. & Kornberg, A. (1993).** Guanosine pentaphosphate
567 phosphohydrolase of *Escherichia coli* is a long-chain exopolyphosphatase. *Proc Natl Acad Sci*
568 *U S A* **90**, 7029-7033.

569 **Keppetipola, N., Jain, R. & Shuman, S. (2007).** Novel triphosphate phosphohydrolase activity
570 of *Clostridium thermocellum* TTM, a member of the triphosphate tunnel metalloenzyme
571 superfamily. *J Biol Chem* **282**, 11941-11949.

572 **Kim, K. S., Rao, N. N., Fraley, C. D. & Kornberg, A. (2002).** Inorganic polyphosphate is
573 essential for long-term survival and virulence factors in *Shigella* and *Salmonella* spp. *Proc Natl*
574 *Acad Sci U S A* **99**, 7675-7680.

575 **Koenig, T., Menze, B. H., Kirchner, M., Monigatti, F., Parker, K. C., Patterson, T., Steen,**
576 **J. J., Hamprecht, F. A. & Steen, H. (2008).** Robust prediction of the MASCOT score for an
577 improved quality assessment in mass spectrometric proteomics. *J Proteome Res* **7**, 3708-3717.

578 **Kohn, G., Delvaux, D., Lakaye, B., Servais, A. C., Scholer, G., Fillet, M., Elias, B.,**
579 **Derochette, J. M., Crommen, J. & other authors (2012).** High inorganic triphosphatase
580 activities in bacteria and mammalian cells: identification of the enzymes involved. *PLoS One* **7**,
581 e43879.

582 **Kornberg, A., Rao, N. N. & Ault-Riche, D. (1999).** Inorganic polyphosphate: a molecule of
583 many functions. *Annu Rev Biochem* **68**, 89-125.

584 **Kristensen, O., Ross, B. & Gajhede, M. (2008).** Structure of the PPX/GPPA phosphatase from
585 *Aquifex aeolicus* in complex with the alarmone ppGpp. *J Mol Biol* **375**, 1469-1476.

586 **Kulaev, I. S., Vagabov, V. M. & Kulakovskaya, T. V. (2005)** *The Biochemistry of Inorganic*
587 *Polyphosphates, 2nd edn.* John Wiley & Sons, Ltd, Chichester, UK.

588 **Kumble, K. D. & Kornberg, A. (1995).** Inorganic polyphosphate in mammalian cells and
589 tissues. *J Biol Chem* **270**, 5818-5822.

590 **Kuroda, A., Murphy, H., Cashel, M. & Kornberg, A. (1997).** Guanosine tetra- and
591 pentaphosphate promote accumulation of inorganic polyphosphate in *Escherichia coli*. *J Biol*
592 *Chem* **272**, 21240-21243.

593 **Larkin, M. A., Blackshields, G., Brown, N. P., Chenna, R., McGettigan, P. A., McWilliam,**
594 **H., Valentin, F., Wallace, I. M., Wilm, A. & other authors (2007).** Clustal W and Clustal X
595 version 2.0. *Bioinformatics* **23**, 2947-2948.

596 **Liao, X. & Butow, R. A. (1993).** RTG1 and RTG2: two yeast genes required for a novel path
597 of communication from mitochondria to the nucleus. *Cell* **72**, 61-71.

598 **Lichko, L. P., Kulakovskaya, T. V. & Kulaev, I. S. (2002).** Two exopolyphosphatases of
599 *Micrococcus phosphovorans*, a polyphosphate-accumulating eubacterium from activated sludge.
600 *Process Biochemistry* **37**, 799-803.

601 **Lichko, L. P., Andreeva, N. A., Kulakovskaya, T. V. & Kulaev, I. S. (2003).**
602 Exopolyphosphatases of the yeast *Saccharomyces cerevisiae*. *FEMS Yeast Res* **3**, 233-238.

603 **Lindner, S. N., Knebel, S., Wesseling, H., Schoberth, S. M. & Wendisch, V. F. (2009).**
604 Exopolyphosphatases PPX1 and PPX2 from *Corynebacterium glutamicum*. *Appl Environ*
605 *Microbiol* **75**, 3161-3170.

606 **Markham, G. D., Hafner, E. W., Tabor, C. W. & Tabor, H. (1980).** S-Adenosylmethionine
607 synthetase from *Escherichia coli*. *J Biol Chem* **255**, 9082-9092.

608 **Mechold, U., Potrykus, K., Murphy, H., Murakami, K. S. & Cashel, M. (2013).** Differential
609 regulation by ppGpp versus pppGpp in *Escherichia coli*. *Nucleic Acids Res* **41**, 6175-6189.

610 **Moeder, W., Garcia-Petit, C., Ung, H., Fucile, G., Samuel, M. A., Christendat, D. &**
611 **Yoshioka, K. (2013).** Crystal structure and biochemical analyses reveal that the *Arabidopsis*
612 triphosphate tunnel metalloenzyme AtTTM3 is a tripolyphosphatase involved in root
613 development. *Plant J* **76**, 615-626.

614 **Moreno, B., Urbina, J. A., Oldfield, E., Bailey, B. N., Rodrigues, C. O. & Docampo, R.**
615 **(2000).** 31P NMR spectroscopy of *Trypanosoma brucei*, *Trypanosoma cruzi*, and *Leishmania*
616 *major*. Evidence for high levels of condensed inorganic phosphates. *J Biol Chem* **275**, 28356-
617 28362.

618 **Muller, F., Mutch, N. J., Schenk, W. A., Smith, S. A., Esterl, L., Spronk, H. M.,**
619 **Schmidbauer, S., Gahl, W. A., Morrissey, J. H. & other authors (2009).** Platelet
620 polyphosphates are proinflammatory and procoagulant mediators in vivo. *Cell* **139**, 1143-1156.

621 **Nikel, P. I., Chavarria, M., Martinez-Garcia, E., Taylor, A. C. & de Lorenzo, V. (2013).**
622 Accumulation of inorganic polyphosphate enables stress endurance and catalytic vigour in
623 *Pseudomonas putida* KT2440. *Microb Cell Fact* **12**, 50.

624 **Nordberg, H., Cantor, M., Dusheyko, S., Hua, S., Poliakov, A., Shabalov, I., Smirnova, T.,**
625 **Grigoriev, I. V. & Dubchak, I. (2014).** The genome portal of the Department of Energy Joint
626 Genome Institute: 2014 updates. *Nucleic Acids Res* **42**, D26-31.

627 **Ogawa, N., Tzeng, C. M., Fraley, C. D. & Kornberg, A. (2000).** Inorganic polyphosphate in
628 *Vibrio cholerae*: genetic, biochemical, and physiologic features. *J Bacteriol* **182**, 6687-6693.

629 **Perez Mato, I., Sanchez del Pino, M. M., Chamberlin, M. E., Mudd, S. H., Mato, J. M. &**
630 **Corrales, F. J. (2001).** Biochemical basis for the dominant inheritance of hypermethioninemia
631 associated with the R264H mutation of the MAT1A gene. A monomeric methionine
632 adenosyltransferase with tripolyphosphatase activity. *J Biol Chem* **276**, 13803-13809.

633 **Pick, U. & Weiss, M. (1991)** Polyphosphate hydrolysis within acidic vacuoles in response to
634 amine-induced alkaline stress in the halotolerant alga *Dunaliella salina*. *Plant Physiol.* **97**,
635 1234-1240.

- 636 **Rangarajan, E. S., Nadeau, G., Li, Y., Wagner, J., Hung, M. N., Schrag, J. D., Cygler, M.**
637 **& Matte, A. (2006).** The structure of the exopolyphosphatase (PPX) from *Escherichia coli*
638 O157:H7 suggests a binding mode for long polyphosphate chains. *J Mol Biol* **359**, 1249-1260.
- 639 **Rao, N. N., Gomez-Garcia, M. R. & Kornberg, A. (2009).** Inorganic polyphosphate: essential
640 for growth and survival. *Annu Rev Biochem* **78**, 605-647.
- 641 **Rashid, M. H. & Kornberg, A. (2000).** Inorganic polyphosphate is needed for swimming,
642 swarming, and twitching motilities of *Pseudomonas aeruginosa*. *Proc Natl Acad Sci U S A* **97**,
643 4885-4890.
- 644 **Reizer, J., Reizer, A., Saier, M. H., Jr., Bork, P. & Sander, C. (1993).** Exopolyphosphate
645 phosphatase and guanosine pentaphosphate phosphatase belong to the sugar kinase/actin/hsp 70
646 superfamily. *Trends Biochem Sci* **18**, 247-248.
- 647 **Rodrigues, C. O., Ruiz, F. A., Vieira, M., Hill, J. E. & Docampo, R. (2002).** An
648 acidocalcisomal exopolyphosphatase from *Leishmania major* with high affinity for short chain
649 polyphosphate. *J Biol Chem* **277**, 50899-50906.
- 650 **Schuddemat, J., de Boo, R., van Leeuwen, C. C., van den Broek, P. J. & van Steveninck, J.**
651 **(1989).** Polyphosphate synthesis in yeast. *Biochim Biophys Acta* **1010**, 191-198.
- 652 **Seidlmayer, L. K., Gomez-Garcia, M. R., Blatter, L. A., Pavlov, E. & Dedkova, E. N.**
653 **(2012).** Inorganic polyphosphate is a potent activator of the mitochondrial permeability
654 transition pore in cardiac myocytes. *J Gen Physiol* **139**, 321-331.
- 655 **Serrano, A., Perez-Castineira, J. R., Baltscheffsky, M. & Baltscheffsky, H. (2007).** H⁺-
656 PPases: yesterday, today and tomorrow. *IUBMB Life* **59**, 76-83.
- 657 **Sethuraman, A., Rao, N. N. & Kornberg, A. (2001).** The endopolyphosphatase gene: essential
658 in *Saccharomyces cerevisiae*. *Proc Natl Acad Sci U S A* **98**, 8542-8547.
- 659 **Shi, X., Rao, N. N. & Kornberg, A. (2004).** Inorganic polyphosphate in *Bacillus cereus*:
660 motility, biofilm formation, and sporulation. *Proc Natl Acad Sci U S A* **101**, 17061-17065.
- 661 **Tammenkoski, M., Koivula, K., Cusanelli, E., Zollo, M., Steegborn, C., Baykov, A. A. &**
662 **Lahti, R. (2008).** Human metastasis regulator protein H-prune is a short-chain
663 exopolyphosphatase. *Biochemistry* **47**, 9707-9713.
- 664 **The UniProt Consortium. (2014).** Activities at the Universal Protein Resource (UniProt).
665 *Nucleic Acids Res* **42**, D191-198.
- 666 **Urech, K., Durr, M., Boller, T., Wiemken, A. & Schwencke, J. (1978).** Localization of
667 polyphosphate in vacuoles of *Saccharomyces cerevisiae*. *Arch Microbiol* **116**, 275-278.
- 668 **Wahlund, T., Woese, C., Castenholz, R. & Madigan, M. (1991).** A thermophilic green sulfur
669 bacterium from New Zealand hot springs, *Chlorobium tepidum* sp. nov. *Arch Microbiol* **156**,
670 81-90.
- 671 **Zhang, H., Gomez-Garcia, M. R., Brown, M. R. & Kornberg, A. (2005).** Inorganic
672 polyphosphate in *Dictyostelium discoideum*: influence on development, sporulation, and
673 predation. *Proc Natl Acad Sci U S A* **102**, 2731-2735.

674 **FIGURE CAPTIONS**

675

676 **Fig. 1.** (a) Electrophoretic analysis of PCR-amplified DNA fragments corresponding to
 677 the *ppx1* and *ppx2* genes of *C. tepidum* TLS. Amplification reactions were performed with
 678 specific primers pairs (Table S1) and bacterial genomic DNA as a template, as described in
 679 Materials and Methods, and subsequently loaded onto 1% (w/v) agarose-TBE gels using
 680 *EcoRI/HindIII*-cleaved lambda phage DNA as a fragment size marker (M). Single major bands
 681 with the expected sizes for *ppx1* and *ppx2*, ca. 1.0 and 1.6 kb respectively, were obtained and
 682 indicated by arrows in the figure. (b) SDS-PAGE analysis of the recombinant CtPPX proteins
 683 expressed in *E. coli*. Samples of cell-free extracts (50 µg) and purified proteins after FPLC gel
 684 filtration (20 µg) were analyzed on a 11% (w/v) SDS-PAGE gel and visualized by staining with
 685 Coomassie Blue R250. Lane 1, total soluble extract from *E. coli* BL21 (pQE-80L-*ppx1*) induced
 686 cells; lane 2, purified His₆-tagged CtPPX1 (37.2-kDa subunit); lane 3, total soluble extract from
 687 *E. coli* BL21 (pQE-80L-*ppx2*) induced cells; lane 4, purified His₆-tagged CtPPX2 (20 µg, 59.9-
 688 kDa subunit). M, protein markers. Molecular mass values in kDa of protein markers are shown
 689 on the left side. Asterisks indicate the major bands of overproduced recombinant protein in cell-
 690 free extracts. Arrowheads denote the single protein band in the purified preparations of
 691 recombinant CtPPX1 and CtPPX2.

692 **Fig. 2.** Gel filtration chromatography analyses of molecular masses and oligomeric
 693 states of the PPX polyPases of *C. tepidum*. (a) 0.5 ml of a purified preparation of recombinant
 694 CtPPX1 were applied to a Superose 12 HR 10/30 column for FPLC gel filtration
 695 chromatography. Calibration curve with protein standards is displayed on the upper left corner
 696 of the graphic. SDS-PAGE analysis of the collected fractions by Coomassie-Blue staining is
 697 shown below. Note that both single chromatographic peaks, corresponding to protein
 698 absorbance at 280 nm (broken line) and polyPase activity with P₁₃₋₁₈ as a substrate (solid line),
 699 co-eluted. (b) 0.5 ml of a purified CtPPX2 preparation were applied to the Superose column and
 700 eluted as described for panel A. Both protein absorbance and polyPase activity also co-eluted as
 701 a single peak in this case. 50-µl aliquots of selected fractions around the central peak fractions
 702 (marked with asterisks) were applied per lane in SDS-PAGE gels. K_{av} and M_m: phase
 703 distribution coefficient and molecular mass of the analyzed proteins, respectively.

704 **Fig. 3.** Catalytic activities of recombinant CtPPX1 and CtPPX2. (a) Influence of polyP
 705 length on the phosphatase activity. The release of Pi by CtPPX1 (black bars) and CtPPX2
 706 (white bars) was determined using 1 mM of polyPs of different chain lengths as substrates. No
 707 significant activity was detected with *p*-nitrophenylphosphate (pNPP), PPi or P_{3c} with any of the
 708 two enzymes. (b) Substrate specificities of NTPase and guanosine tetrphosphatase activities.
 709 Phosphatase activity levels were determined with 1 mM NTPs or GP₄. NTPase and polyPase
 710 activities were measured as described in Materials and Methods. (c) Metal cofactor specificity
 711 of CtPPX1 and CtPPX2. PolyPase activity towards P₃ (CtPPX1, black bars), or P_{LC} (CtPPX2,
 712 white bars) in the presence of 5 mM of divalent cations cofactors. 100% value assigned to the
 713 optimum cofactor Mg²⁺ corresponds to 591 ± 37 µmol min⁻¹ mg⁻¹ and 125 ± 12 µmol min⁻¹ mg⁻¹
 714 for CtPPX1 and CtPPX2, respectively. A drastic reduction in enzyme activity was observed in
 715 the presence of an excess of the chelating agent EDTA. N.A. lane, no addition of divalent
 716 cation. No detectable activities were found in the presence of EDTA with no addition of
 717 divalent cation (not shown). All data are shown as means ± S.E. obtained from three
 718 independent experiments. The limit of detection was ca. 0.004 µmol min⁻¹ mg⁻¹.

719 **Fig. 4.** pH profile curve and polyPase activity of recombinant CtPPX1 and CtPPX2
720 proteins. Dependence on pH for the polyPase activity in the presence of 5 mM MgCl₂ at 30 °C
721 of purified recombinant CtPPX1(●) with P₃, CtPPX1(▲) with P₁₃₋₁₈, and CtPPX2 (○) P_{LC} as
722 substrate, respectively. Note both enzymes exhibit a well defined activity peak around pH 6.5.
723 100% levels correspond to 587 ± 39, 166 ± 7 and 125 ± 10 μmol min⁻¹ mg⁻¹ for CtPPX1 with P₃
724 and P₁₃₋₁₈ as substrates and CtPPX2 with P_{LC} as substrate, respectively. Values are means of
725 three independent experiments and bars indicate S.E.

726 **Fig. 5.** Molecular phylogenetic analysis of the two CtPPX paralogs of *C. tepidum* and
727 their evolutionary relationships with Ppx-GppA proteins of other prokaryotes (archaea and
728 bacteria), fungi, protists and metazoa. Amino acid sequences obtained from GenBank (Benson
729 *et al.*, 2013), JGI genome database (Nordberg *et al.*, 2014) and Cyanobase (Fujisawa *et al.*,
730 2014) were used to construct a multiple sequences alignment with CLUSTAL X software tool
731 (Larkin *et al.*, 2007) and a evolutionary distance tree (Neighbor-joining method) was eventually
732 constructed with Seaview software (Gouy *et al.*, 2010). Protein sequences are represented by
733 their UniprotKG (The UniProt Consortium, 2014) entry names. Numbers above lines show
734 bootstrap percentages (based on 1000 replicates) supporting sequences groups representing
735 main Ppx-GppA protein families (shaded grey). Scale bar represents number of amino acid
736 changes per site. Archaeal and eukaryotic sequences, all the latest in the cluster of RTG2
737 proteins, are in bold. Biochemically characterized proteins are shown boxed and sequences of
738 phototrophic microorganisms are italicized. Note the general occurrence of pairs of CtPPX-like
739 paralogs among the Chlorobia species, suggesting that it could be a characteristic feature for this
740 phylogenetic clade. Paralogous pairs involving members of different Ppx-GppA protein
741 subfamilies occur in diverse bacterial species, and are indicated by a range of symbols
742 (diamonds, triangles, squares, asterisks, crosses). Pairs of close paralogs located in the same
743 cluster of sequences suggesting recent gene duplication events are indicated by a **D**. A list of
744 UniprotKG entries, organism phylogenies and domain architectures of the Ppx-GppA proteins
745 used for this study is shown in Table S3.

746

747 **TABLES**

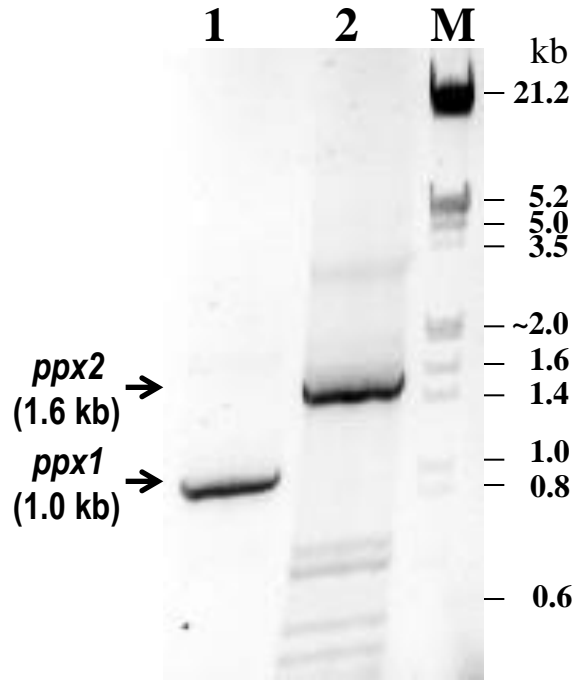
748

749 **Table 1.** Some physico-chemical and catalytic properties of the recombinant polyphosphatases
750 PPX1 and PPX2 from *C. tepidum* TLS

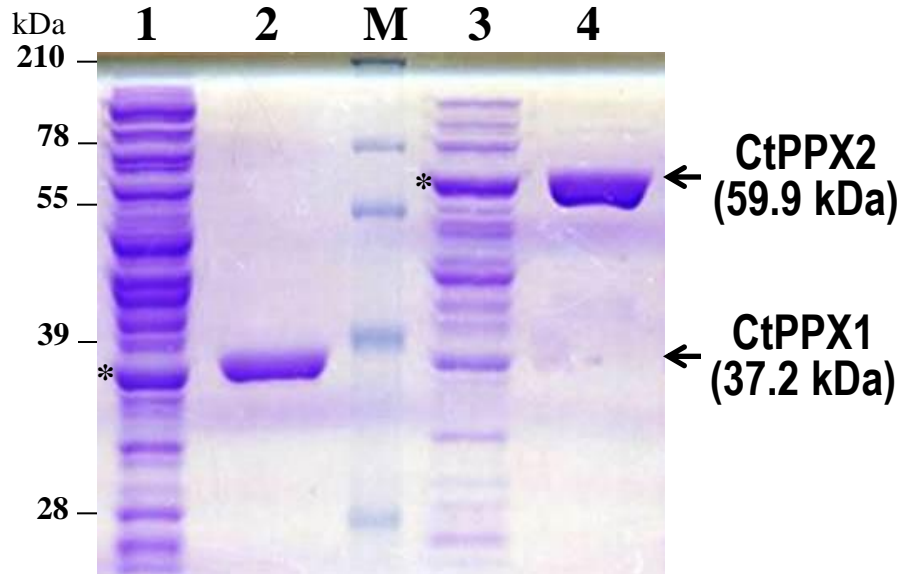
Properties	CtPPX1	CtPPX2
Molecular mass M_m (kDa)		
Native oligomer (FPLC)	38.8	100.4
Subunit (SDS-PAGE)	37.2	59.9
Oligomeric state	monomer	homodimer
Optimum pH	6.5	6.5
Domain architecture	Ppx-GppA	Ppx-GppA - HD
Optimum metal cofactor	Mg^{2+}	Mg^{2+}
Preferred substrate	short-chain polyP (P_3)	long-chain polyP
P_3 kinetic parameters*		
K_m (μM)	97.7 ± 9.0	212.9 ± 19.4
V_{max} ($\mu mol\ min^{-1}\ mg^{-1}$)	643.1 ± 44.9	6.8 ± 0.4
k_{cat} (s^{-1})	398.7 ± 15.6	13.5 ± 3.3
Catalytic efficiency k_{cat}/K_m ($mM^{-1}\ s^{-1}$)	$4,081 \pm 78$	63 ± 6
GP_4 kinetic parameters¹		
K_m (μM)	242.2 ± 20.8	335.5 ± 23.5
V_{max} ($\mu mol\ min^{-1}\ mg^{-1}$)	497.4 ± 23.6	7.1 ± 0.2
k_{cat} (s^{-1})	308.4 ± 38.9	14.2 ± 1.4
Catalytic efficiency k_{cat}/K_m ($mM^{-1}\ s^{-1}$)	$1,273 \pm 66$	42 ± 6
P_{13-18} kinetic parameters¹		
K_m (μM)	597.4 ± 68.6	264.4 ± 12.4
V_{max} ($\mu mol\ min^{-1}\ mg^{-1}$)	245.6 ± 9.1	227.3 ± 11.3
k_{cat} (s^{-1})	157.0 ± 7.9	453.8 ± 37.4
Catalytic efficiency k_{cat}/K_m ($\mu M^{-1}\ s^{-1}$)	263 ± 10	$1,716 \pm 134$

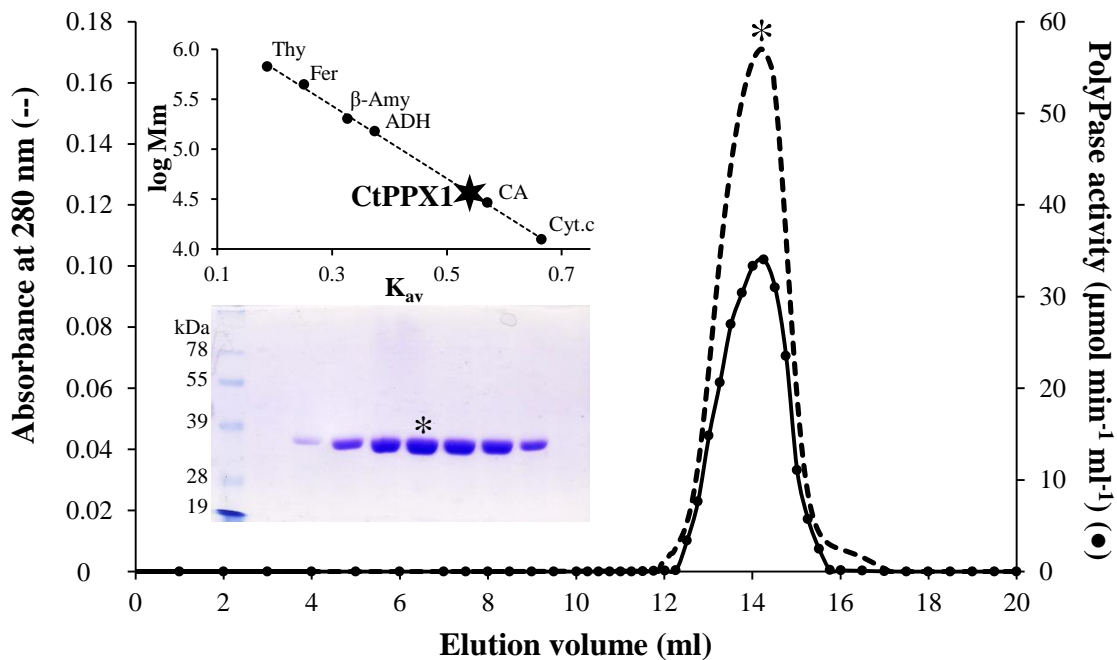
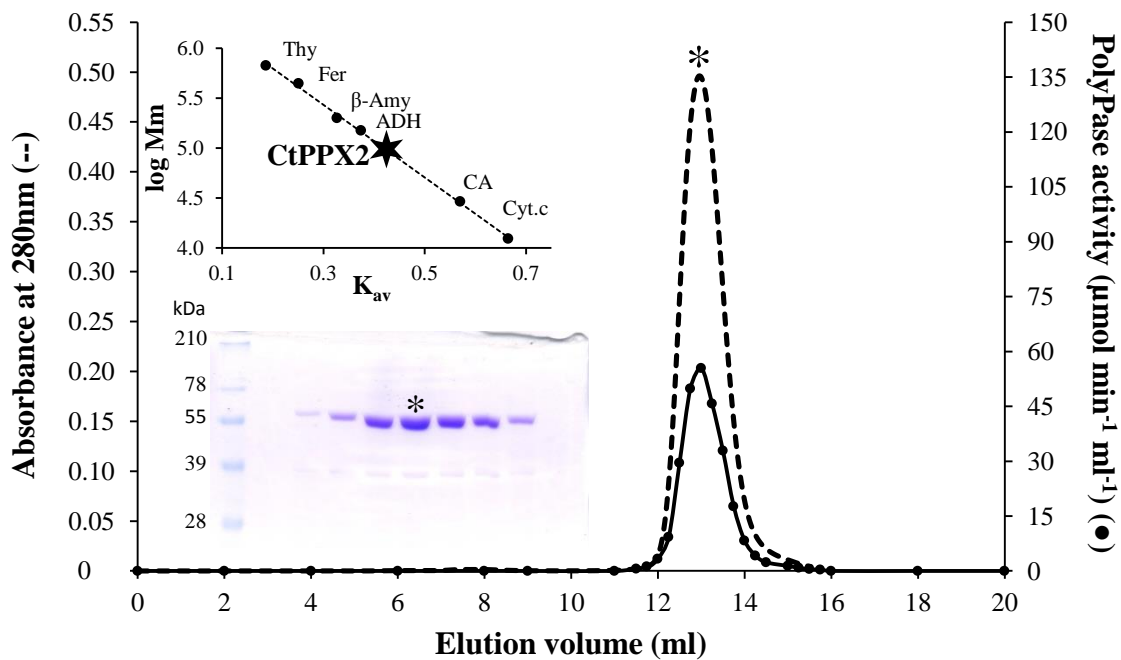
751 * Kinetic parameters were determined by nonlinear curve fitting from the Michaelis-Menten plot using the spreadsheet
752 Anemona.xlt (Hernandez & Ruiz, 1998). When indicated data are means \pm standard errors of three independent determinations.

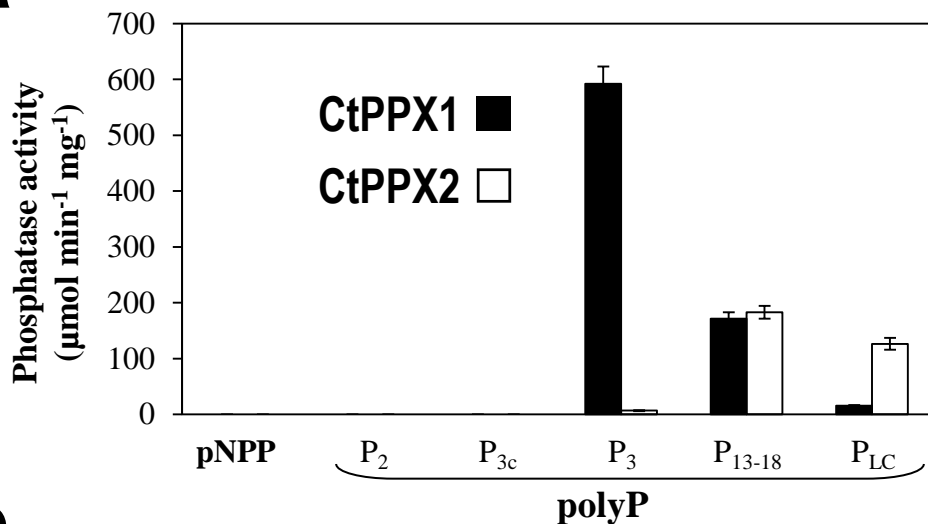
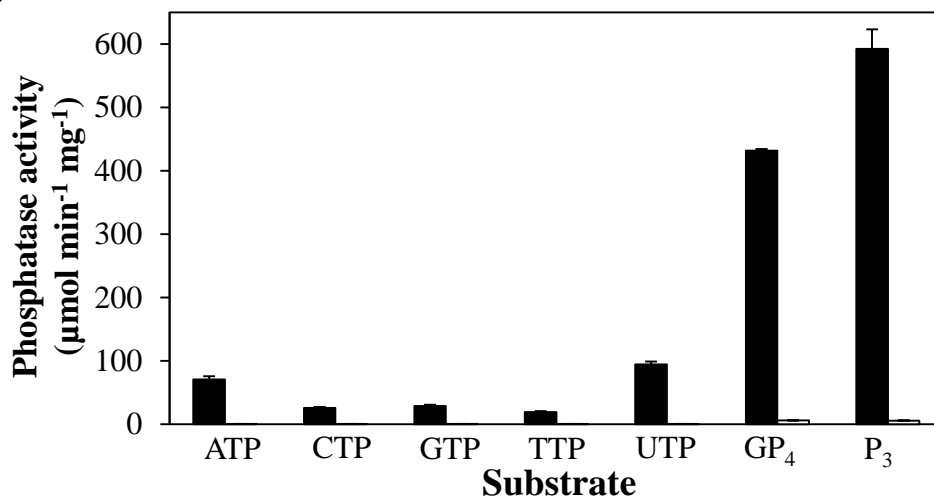
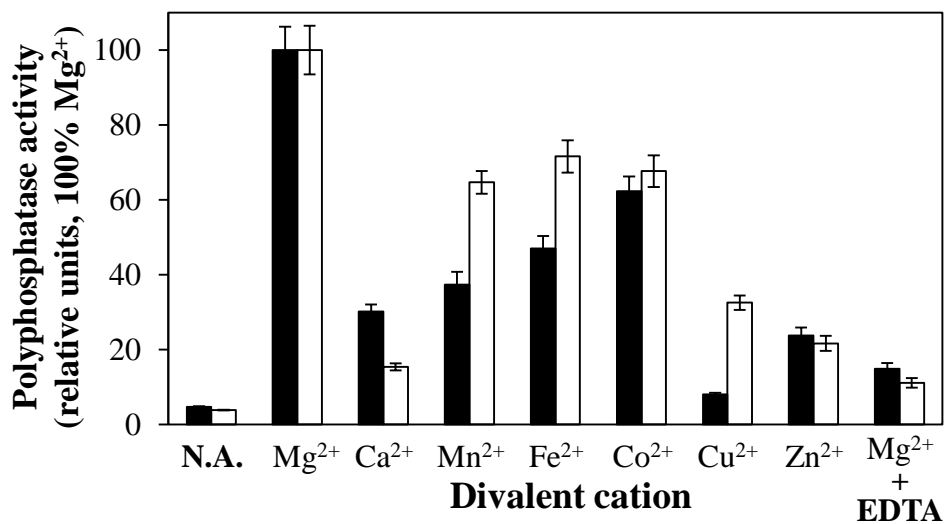
a

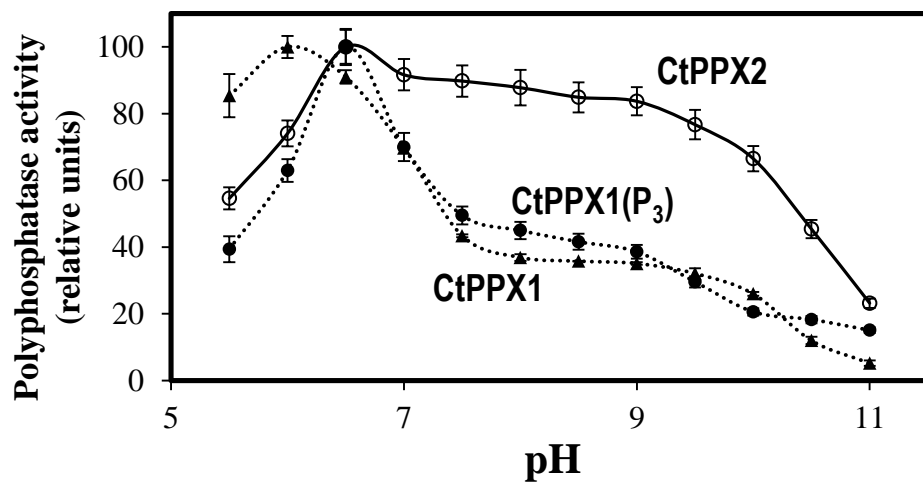


b



a**b**

a**b****c**



High M_m polyPases (500-550 aa) *

Low M_m polyPases (II) (300-500 aa)

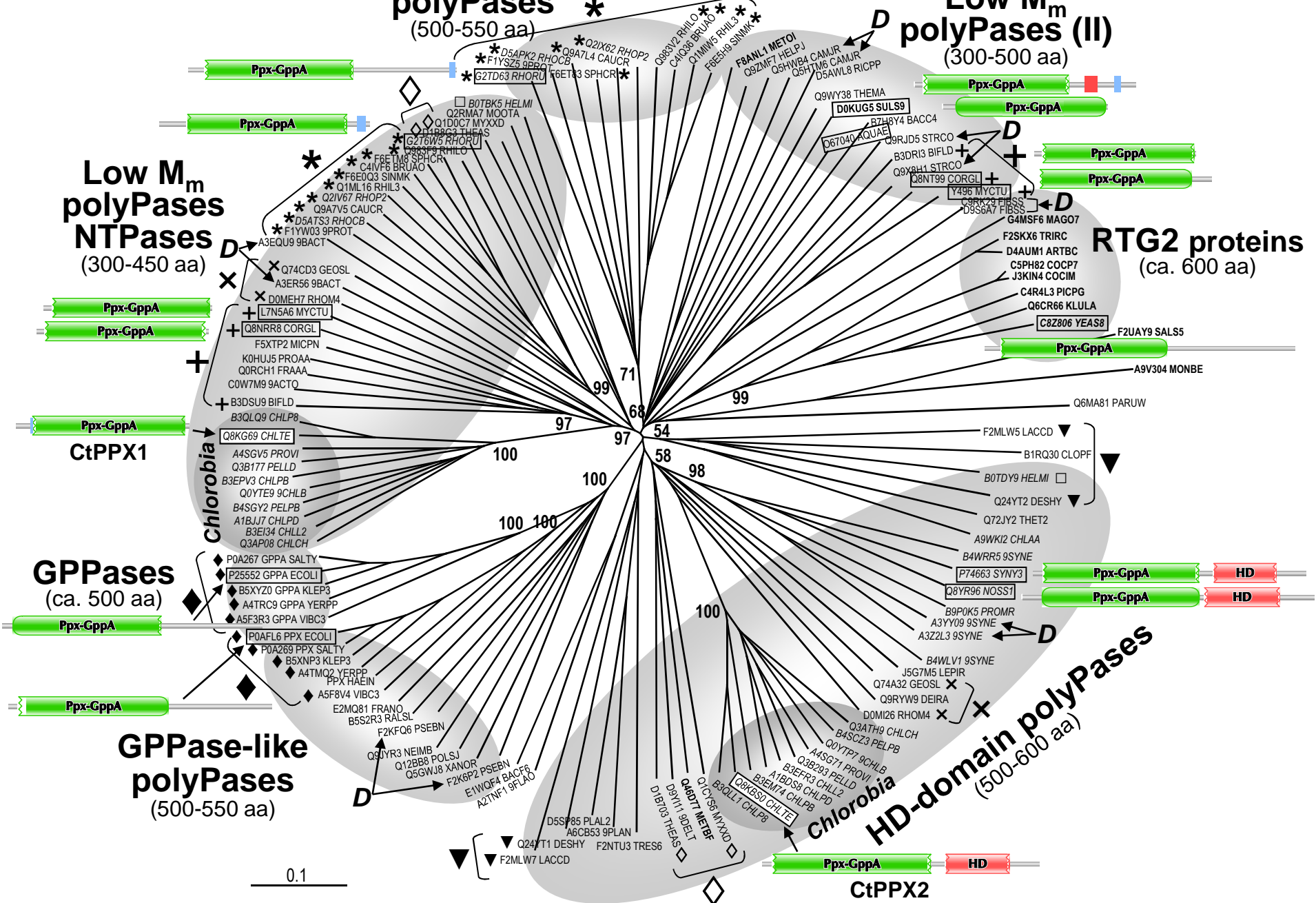
Low M_m polyPases NTPases (300-450 aa)

RTG2 proteins (ca. 600 aa)

GPPases (ca. 500 aa)

GPPase-like polyPases (500-550 aa)

HD-domain polyPases (500-600 aa)



1 **Two Exopolyphosphatases with Distinct Molecular Architectures and Substrate**
2 **Specificities from the Thermophilic Green-sulfur Bacterium *Chlorobium tepidum* TLS**

3 *Tomás Albi & Aurelio Serrano**

4 Instituto de Bioquímica Vegetal y Fotosíntesis, Centro de Investigaciones Científicas Isla
5 Cartuja, CSIC-Universidad de Sevilla, Spain

6 *Corresponding author: Aurelio Serrano, Institute for Plant Biochemistry and Photosynthesis,
7 CSIC and University of Seville- 49th Americo Vespucio Avenue, 41092 Seville, Spain.
8 Telephone: +34 954 460 465; Fax: +34 954 460 165; E-mail: aurelio@ibvf.csic.es

9
10
11
12
13 **SUPPLEMENTARY MATERIAL**

14
15 **Fig. S1.** Multiple protein sequences alignment of the two Ppx-GppA polyPases of *C. tepidum*
16 TLS.

17 **Fig. S2.** Ni-chelate affinity chromatography of the two polyPases of *C. tepidum* TLS
18 heterologously expressed in *E. coli*.

19 **Fig. S3.** Sequence and domain structure validation of *C. tepidum* polyPases using tryptic-
20 peptide fingerprinting and MALDI-TOF mass spectrometry analysis.

21 **Fig. S4.** Kinetic characterization of recombinant CtPPX1.

22 **Fig. S5.** Kinetic characterization of recombinant CtPPX2.

23 **Fig. S6.** Organization of the genomic regions (ca. 5 kb) around the *ppx1* (CT0099) and *ppx2*
24 (CT1713) genes in the genome of *C. tepidum* TLS, and the corresponding regions in the
25 genomes of two closely related species of Chlorobia.

26 **Table S1.** Primers for cloning the *ppx1* and *ppx2* genes from *Chlorobium tepidum* TLS.

27 **Table S2.** Amino acid identities shared between CtPPX1, CtPPX2 and the bacterial Ppx-GppA
28 phosphatases used for the protein alignment shown in Figure S1.

29 **Table S3.** Sequences of Ppx-GppA proteins displayed in the phylogenetic tree of Figure 5

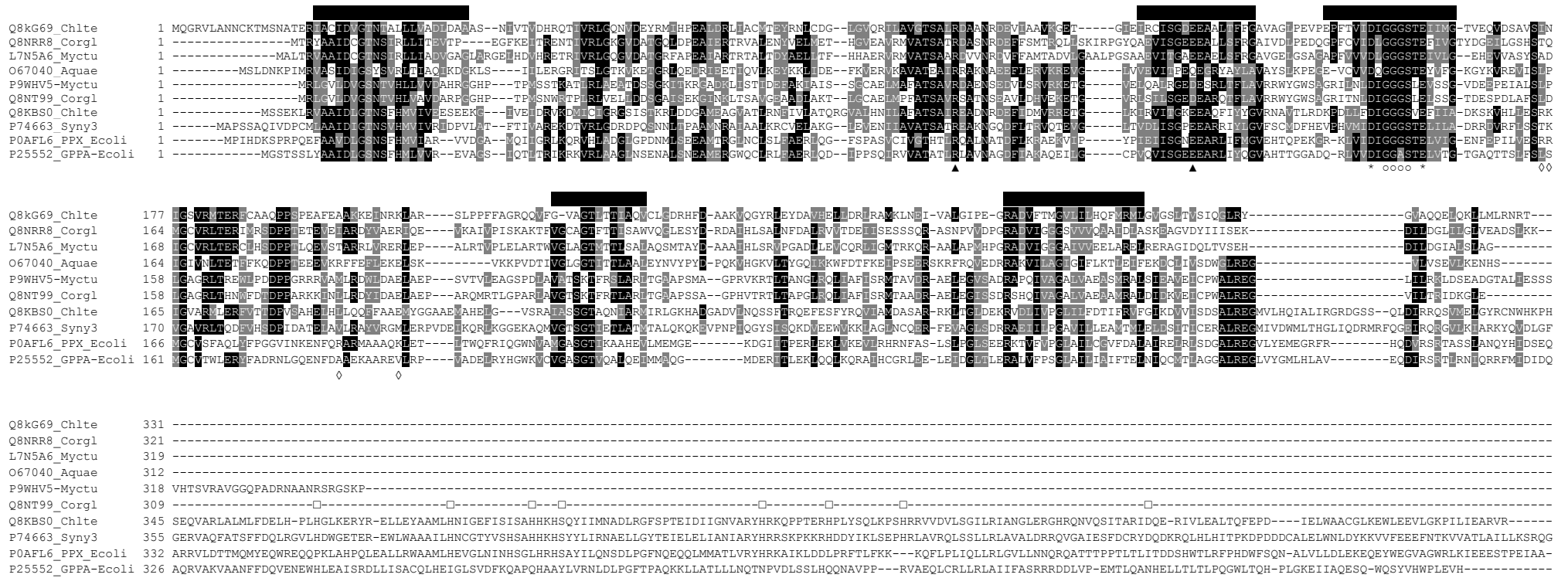
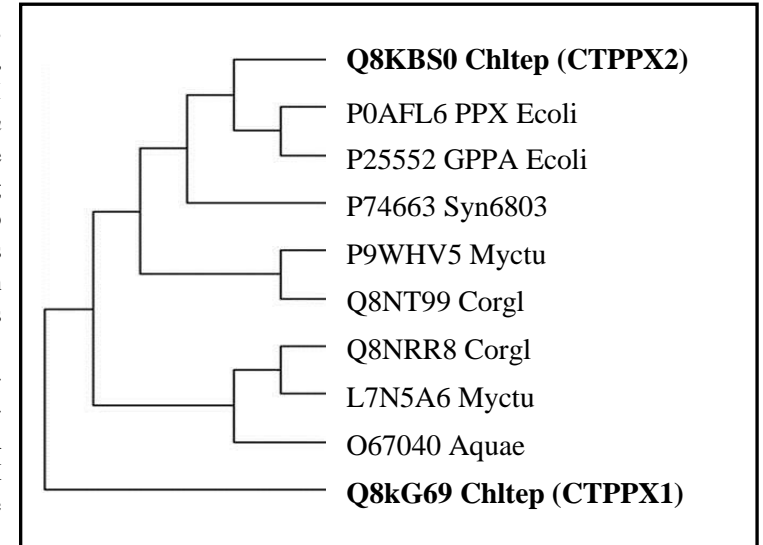


Fig. S1. Multiple protein sequences alignment of the two Ppx-GppA polyPases of *C. tepidum* TLS (Q8KG69_CHLTE, CtPPX1; Q8KBS0_CHLTE, CtPPX2), the Ppx-GppA phosphatase of *Aquifex aeolicus* (O67040_AQUAE) (Kristensen *et al.*, 2008), the PPX of *Synechocystis* sp. PCC6803 (P74663_SYNY3) (Albi T. and Serrano A., unpublished), the pairs of PPX paralogs of *Corynebacterium glutamicum* (Q8NRR8_CORGL; Q8NT99_CORGL) (Lindner *et al.*, 2009) and *Mycobacterium tuberculosis* (L7N5A6_MYCTU; Y496_MYCTU) (Choi *et al.*, 2012), and the polyPase (PPX_ECOLI) and guanosine pentaphosphatase (GPPA_ECOLI) of *E. coli* (Rangarajan *et al.*, 2006). UniProtKG retrieved sequences were aligned using CLUSTAL X, then manually curated, and the final alignment was formatted with the ExPASy BoxShade server. The two catalytic residues Arg and Glu (Arg93 and Glu121 in *E. coli* PPX, marked by triangles), two metal-cofactor coordinating sites (Asp143 and Glu150 in *E. coli* PPX, indicated by asterisks) and the phosphate-binding glycine-rich loop (Gly145-Ser148 in *E. coli* PPX, indicated by a set of white circles) are highly conserved. In contrast, a number of polyP-binding basic residues reported in *E. coli* PPX (indicated by white diamonds) do not show a clear conservation pattern in the examined sequences. Noteworthy, the five regions of the ATPase fold characteristic of the sugar kinase/actin/hsp70 superfamily to which the Ppx-GppA protein family belong (marked by thick black dashes at the top) show significant levels of conservation. Note the C-terminal extra regions of CtPPX2, the cyanobacterial PPX of *Synechocystis* and the two Ppx-GppA phosphatases of *E. coli*. A number of amino acid residues (mostly His) characteristic of the C-terminal HD domain of CtPPX2 and *Synechocystis* PPX are marked by open squares. The inset shows a parsimony phylogram (100 replicates) of the protein sequences used for the alignment in which the two CtPPXs clearly arrange in different clusters.



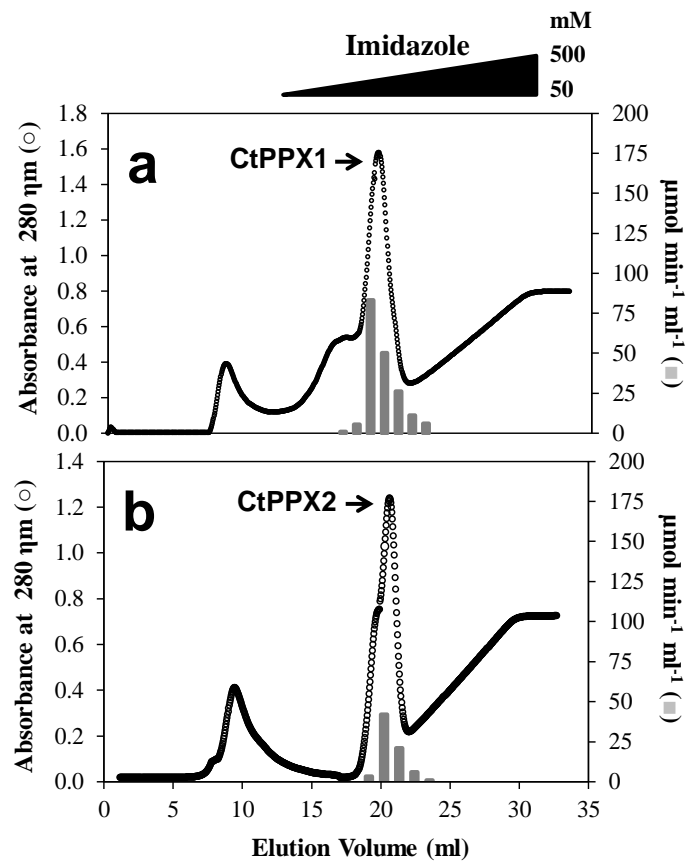


Fig. S2. Ni-chelate affinity chromatography of the two polyPases of *C. tepidum* TLS heterologously expressed in *E. coli*. Sonicated *E. coli* BI21 (DE3) cells overexpressing CtPPX1 (panel A) or CtPPX2 (panel B) were centrifuged and the crude extracts (soluble protein fraction) containing polyPase activities were loaded onto a pre-equilibrated HisTrap[®] HP 1 ml Ni-NTA column. Partially purified recombinant PPX proteins (>95% purity) were eluted using a linear gradient of imidazole with a target concentration of 500 mM. Elution was monitored by registering absorbance at 280 nm and aliquots of fractions were taken to check for polyPase activity.

aa: 1 33 323 330



{MATRIX} Mascot Search Results

{SCIENCE} Probability Based Mowse Score

Match to: **gi|21672940**
Exopolyphosphatase, putative [Chlorobium tepidum TLS] CtPPX1
 Sequence coverage of natural protein: **60 %**
 Nominal mass (M_r): **35,799 (without the N-terminal His-tag of 12 aa)**

1	mrqshhhhhh	gsMQGRVLAN	NCKTMSNATE	RIACIDVGTN	TALLLVADLD
51	AAASNIVTVD	HRQTIIVRLGQ	NVDEYRMIHP	EALDRLIACM	TEYRNLCDGL
101	GVQRILAVGT	SALRDAANRD	EVIAAVKGET	GIEIRCISGD	EEAALTFFGA
151	VAGLPEVPEP	FTVIDIGGGS	TEIIMGTVEQ	VDSAVSINIG	SVRMTERFCA
201	AQPPSPEAFE	AAKKEINRKL	ARSLPPFFAG	RQQVFGVAGT	LTTIAQVCLG
251	DRHFDAAKVQ	GYRLEYDAVH	ELLDRLRAMK	LNEIVALGIP	EGRADVFTMG
301	VLIILHQFMRM	LGVGSITVSI	QGLRYGVAQQ	ELQKLLMLRN	RT

aa: 1 20 315 344 462 518



{MATRIX} Mascot Search Results

{SCIENCE} Probability Based Mowse Score

Match to: **gi|21674530**
Exopolyphosphatase, putative [Chlorobium tepidum TLS] CtPPX2
 Sequence coverage of natural protein: **50 %**
 Nominal mass (M_r): **58,436 (without the N-terminal His-tag of 12 aa)**

1	mrqshhhhhh	gsMSSEKLRV	AAIDLGTNSF	HMVIVEESE	KGIVEIDRVK
51	DMICIGRGS	STKRLDDGAM	EAGVATLRNF	IVLATQRGVA	LHNILAFATS
101	AIREADNRDE	FIDMVRRETG	LKIRVITGKE	EAQFIYYGVR	NAVTLRDKPD
151	LLFDIGGGSV	EFIIADKSKV	HLLESRKIGV	ARMLERFVTT	DPVSAHELHL
201	LQOFFAAEMY	GGAEMAHEL	GVSRAIASSG	TAQNIARMIR	LGKHADGADV
251	LNQSSFTRQE	FESFYRQVIA	MDASARRKLT	GLDEKRVDLI	VPGLILFDTI
301	FRVFGIKDVV	ISDSALREGM	VLHQIALIRG	RDGSSQLDIR	RQSVMEELGYR
351	CNWHKPHEQ	VARLALMLFD	ELHPLHGLKE	RYRELLEYAA	MLHNIGEFIS
401	ISAHKHSQY	IIMNADLRGF	SPTEDIIGN	VARYHRKQPP	TERHPLYSQL
451	KPSHRRVVDV	LSGILRIANG	LERGHRQNVQ	SITARIDQER	IVLEALTQFE
501	PDIELWAACG	LKEWLEEVLG	KPILIEARVR		

Fig. S3. Sequence and domain structure validation of *C. tepidum* polyPases using tryptic-peptide fingerprinting and MALDI-TOF mass spectrometry analysis. The Pfam domain structures of the two natural CtPPX proteins are shown, as well as the sequences of the corresponding purified recombinant proteins in which amino acid residues are bold-colored accordingly, the experimentally identified peptides are underlined and the N-terminal His-tags are in lowercase. Identified peptides cover about 60 and 50 % of the predicted protein sequences of natural CtPPX1 and CtPPX2, respectively

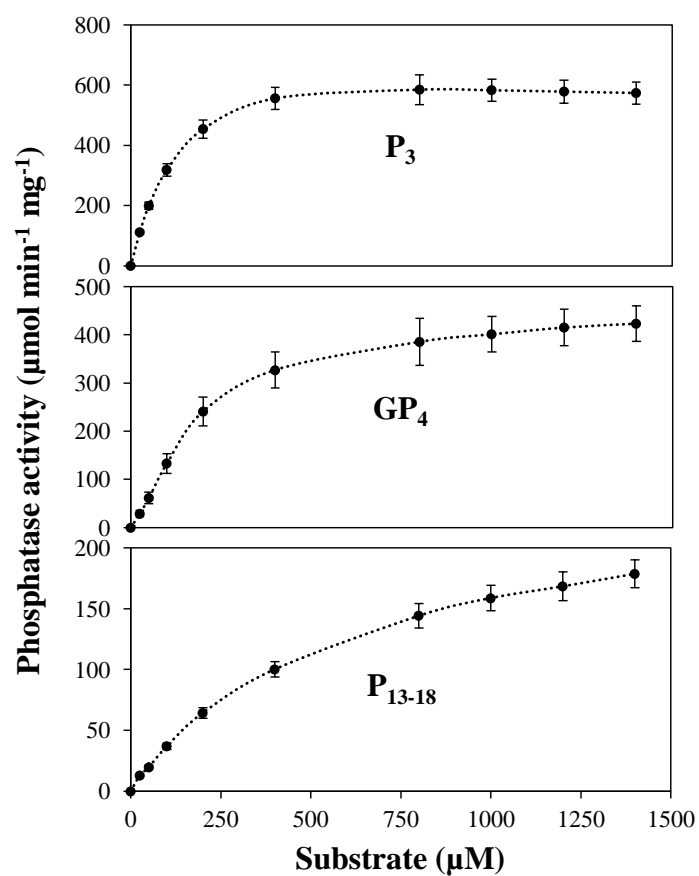


Fig. S4. Kinetic characterization of recombinant CtPPX1. A substrate concentration curve was constructed, and enzyme catalytic parameters (apparent K_m , V_{max} and k_{cat}) were determined for P₃ (A), GP₄ (B), and P₁₃₋₁₈ (C) (summarized in Table 1). All assays were performed in triplicate at 30 °C.

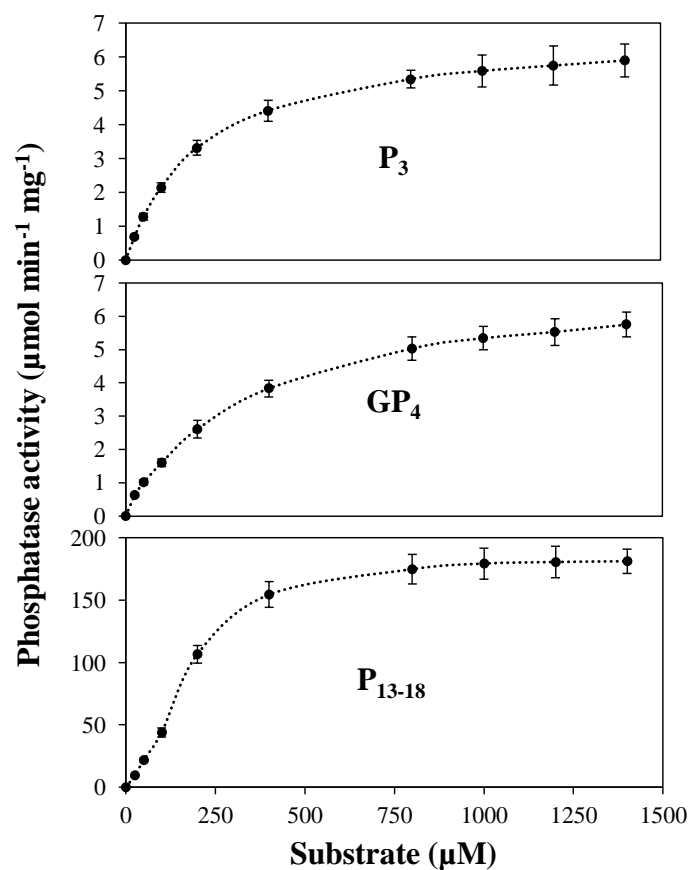


Fig. S5. Kinetic characterization of recombinant CtPPX2. A substrate concentration curve was constructed, and enzyme catalytic parameters (apparent K_m , V_{\max} and k_{cat}) were determined for P₃ (A), GP₄ (B), and P₁₃₋₁₈ (C) (summarized in Table 1). All assays were performed in triplicate at 30 °C.

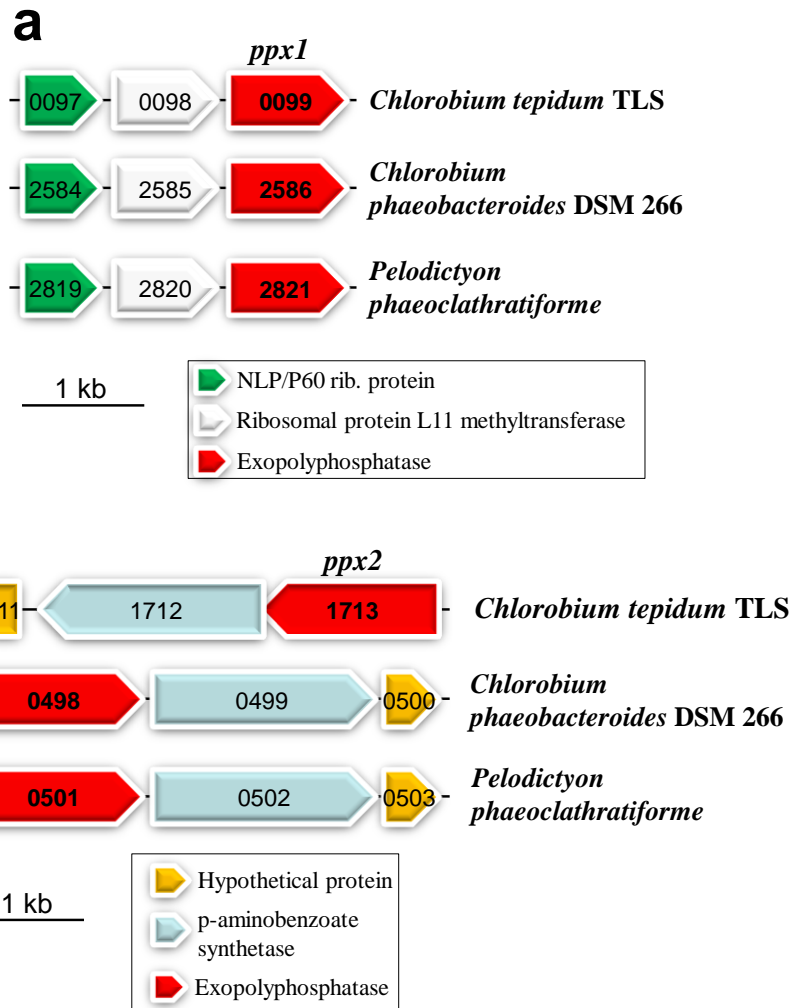


Fig. S6. Organization of the genomic regions (ca. 5 kb) around the *ppx1* (CT0099) and *ppx2* (CT1713) genes in the genome of *C. tepidum* TLS, and the corresponding regions in the genomes of two closely related species of Chlorobia. Sequence data were obtained from the JGI Integrated Microbial Genomes Portal (<http://img.jgi.doe.gov/>). Note the occurrence of *ppx1* and *ppx2* genes in hypothetical operons located in quite distant regions of the bacterial genome. While *ppx1* is located in a gene cluster downstream two genes encoding ribosomal proteins (50S ribosomal protein L11 methyltransferase and NLP/P60 ribosomal protein), the *ppx2* gene cluster with two genes encoding a *p*-aminobenzoate synthetase and a hypothetical protein. These genomic architectures are conserved in all genomes of Chlorobia/Bacteroidetes species sequenced so far.

Table S1. Primers for cloning the *ppx1* and *ppx2* genes from *Chlorobium tepidum* TLS

Gene	Primers (new restriction site, underlined)	
<i>ppx1</i> (CT0099)	F (<i>Bam</i> HI)	5'-TTAGGATCCATGCAAGGTCCGGGTTCTCG-3'
	R (<i>Pst</i> I)	5'-TTACTGCAGTCAGGTCCGGTTGCGAAGC-3'
<i>ppx2</i> (CT1713)	F (<i>Bam</i> HI)	5'-GCAGGATCCATGTCATCAGAGAAACTCAGG-3'
	R (<i>Pst</i> I)	5'-TTACTGCAGTTACCGGACGCGGGCTTCG-3'

Table S2. Amino acid identities shared between CtPPX1, CtPPX2 and the bacterial Ppx-GppA phosphatases used for the protein alignment shown in Figure S1

Protein and Gene codes	Accession number Organism	CtPPX1 Q8KG69 Identities (%)	CtPPX2* Q8KBS0 Identities (%)
CtPPX1 (330 aa) <i>Ct0099</i>	Q8KG69 <i>Chlorobium tepidum</i>	--	27
CtPPX2* (518 aa) <i>Ct1713</i>	Q8KBS0 <i>Chlorobium tepidum</i>	27	--
PPX1 (309 aa) <i>Cg0488</i>	Q8NT99 <i>Corynebacterium glutamicum</i>	28	28
PPX2 (321 aa) <i>Cg1115</i>	Q8NRR8 <i>Corynebacterium glutamicum</i>	35	28
Rv0496 (MTB-PPX1) <i>MT0516</i> (344 aa)	P9WHV5_MYCTU <i>Mycobacterium tuberculosis</i>	26	25
Rv1026 (319 aa) <i>MT1054</i>	L7N5A6_MYCTU <i>Mycobacterium tuberculosis</i>	37	25
AaPPX (312 aa)	O67040 <i>Aquifex aeolicus</i>	29	25
SyPPX* (540 aa) <i>sll1546</i>	P74663 <i>Synechocystis sp. PCC6803</i>	29	35
EcPPX (531 aa)	P0AFL6 <i>Escherichia coli</i>	28	27
EcGPPA (494 aa)	P25552 <i>Escherichia coli</i>	29	27

Highest values of amino acid identities are shown in bold.

* PolyPases with a two-domain architecture PpxGppA-HD.

Table S3. Sequences of Ppx-GppA proteins displayed in the phylogenetic tree of Figure 5

UniProtKB	Organism	Subfamily	Phylogeny	Reference
Q8KBS0	<i>Chlorobium tepidum</i> TLS	PolyPase-HD	Chlorobia	This study
Q8KG69	<i>Chlorobium tepidum</i> TLS	Low M _m polyPase I	Chlorobia	This study
A4SG71	<i>Prosthecochloris vibrioformis</i> DSM 265	PolyPase-HD	Chlorobia	
A4SGV5	<i>Prosthecochloris vibrioformis</i> DSM 265	Low M _m polyPase I	Chlorobia	
B3EFR3	<i>Chlorobium limicola</i> DSM 245	PolyPase-HD	Chlorobia	
B3EI34	<i>Chlorobium limicola</i> DSM 245	Low M _m polyPase I	Chlorobia	
B3EM74	<i>Chlorobium phaeobacteroides</i> BS1	PolyPase-HD	Chlorobia	
B3EPV3	<i>Chlorobium phaeobacteroides</i> BS1	Low M _m polyPase I	Chlorobia	
B3QLL1	<i>Chlorobaculum parvum</i> NCIB 8327	PolyPase-HD	Chlorobia	
B3QLQ9	<i>Chlorobaculum parvum</i> NCIB 8327	Low M _m polyPase I	Chlorobia	
Q3ATH9	<i>Chlorobium chlorochromatii</i> CaD3	PolyPase-HD	Chlorobia	
Q3AP08	<i>Chlorobium chlorochromatii</i> CaD3	Low M _m polyPase I	Chlorobia	
A1BDS8	<i>Chlorobium phaeobacteroides</i> DSM 266	PolyPase-HD	Chlorobia	
A1BJJ7	<i>Chlorobium phaeobacteroides</i> DSM 266	Low M _m polyPase I	Chlorobia	
Q3B293	<i>Pelodictyon luteolum</i> DSM 273	PolyPase-HD	Chlorobia	
Q3B177	<i>Pelodictyon luteolum</i> DSM 273	Low M _m polyPase I	Chlorobia	
B4SCZ3	<i>Pelodictyon phaeoclathratiforme</i> DSM 5477	PolyPase-HD	Chlorobia	
B4SGY2	<i>Pelodictyon phaeoclathratiforme</i> DSM 5477	Low M _m polyPase I	Chlorobia	
Q0YTP7	<i>Chlorobium ferrooxidans</i> DSM 13031	PolyPase-HD	Chlorobia	
Q0YTE9	<i>Chlorobium ferrooxidans</i> DSM 13031	Low M _m polyPase I	Chlorobia	
B0TDY9	<i>Heliobacterium modesticaldum</i> ATCC 51547	PolyPase-HD	Clostridia	
B0TBK5	<i>Heliobacterium modesticaldum</i> ATCC 51547	Low M _m polyPase I	Clostridia	
Q1CYS6	<i>Myxococcus xanthus</i> DK 1622	PolyPase-HD	δ proteobacteria, Myxococcales	
Q1D0C7	<i>Myxococcus xanthus</i> DK 1622	Low M _m polyPase I	δ proteobacteria, Myxococcales	
Q74A32	<i>Geobacter sulfurreducens</i> ATCC 51573	PolyPase-HD	δ proteobacteria, Desulfuromonadales	
Q74CD3	<i>Geobacter sulfurreducens</i> ATCC 51573	Low M _m polyPase I	δ proteobacteria, Desulfuromonadales	
D0MI26	<i>Rhodothermus marinus</i> ATCC 43812	PolyPase-HD	Bacteroidetes	
D0MEH7	<i>Rhodothermus marinus</i> ATCC 43812	Low M _m polyPase I	Bacteroidetes	
D1B703	<i>Thermanaerovibrio acidaminovorans</i> ATCC 49978	PolyPase-HD	Synergistetes	
D1B8G3	<i>Thermanaerovibrio acidaminovorans</i> ATCC 49978	Low M _m polyPase I	Synergistetes	
P74663	<i>Synechocystis</i> sp. PCC 6803	PolyPase-HD	Cyanobacteria	Albi T. and Serrano A., unpublished
Q8YR96	<i>Nostoc</i> sp. PCC 7120	PolyPase-HD	Cyanobacteria	Albi T. and Serrano A., unpublished
A3YY09	<i>Synechococcus</i> sp. WH 5701	PolyPase-HD (D)	Cyanobacteria	
A3Z2L3	<i>Synechococcus</i> sp. WH 5701	PolyPase-HD cluster(D)	Cyanobacteria	
B4WLV1	<i>Synechococcus</i> sp. PCC 7335	PolyPase-HD	Cyanobacteria	
B4WRR5	<i>Synechococcus</i> sp. PCC 7335	PolyPase-HD	Cyanobacteria	
B9P0K5	<i>Prochlorococcus marinus</i> MIT 9202	PolyPase-HD	Cyanobacteria	
A9WKI2	<i>Chloroflexus aurantiacus</i> ATCC 29366	PolyPase-HD	Chloroflexi	
Q9RYW9	<i>Deinococcus radiodurans</i> ATCC 13939	PolyPase-HD	Deinococcus-Thermus group	
Q72JY2	<i>Thermus thermophilus</i> ATCC BAA-163	PolyPase-HD	Deinococcus-Thermus group	
D5SP85	<i>Planctomyces limnophilus</i> ATCC 43296	PolyPase-HD	Planctomycetes	
A6CB53	<i>Planctomyces maris</i> DSM 8797	PolyPase-HD	Planctomycetes	

F2NTU3	<i>Treponema succinifaciens</i> ATCC 33096	PolyPase-HD	Spirochaetes	
J5G7M5	<i>Leptospira interrogans</i> FPW2026	PolyPase-HD	Spirochaetes	
D9Yi11	<i>Desulfovibrio sp. 3_1_syn3</i>	PolyPase-HD	δ proteobacteria, Desulfovibrionales	
Q24YT1	<i>Desulfotobacterium hafniense</i> Y51	PolyPase-HD	Clostridia	
Q24YT2	<i>Desulfotobacterium hafniense</i> Y51	PolyPase-HD	Clostridia	
F2MLW7	<i>Lactobacillus casei</i> BD-II	PolyPase-HD	Bacilli	
F2MLW5	<i>Lactobacillus casei</i> BD-II	PolyPase-HD cluster	Bacilli	
B1RQ30	<i>Clostridium perfringens</i> NCTC 8239	PolyPase-HD cluster	Clostridia	
A2TNF1	<i>Dokdonia donghaensis</i> MED134	PolyPase-HD cluster	Flavobacteria	
E1WQF4	<i>Bacteroides fragilis</i> 638R	PolyPase-HD cluster	Bacteroidetes	
A3EQU9	<i>Leptospirillum rubarum</i>	Low M _m polyPase I (D)	Nitrospirae	
A3ER56	<i>Leptospirillum rubarum</i>	Low M _m polyPase I (D)	Nitrospirae	
C0W7M9	<i>Actinomyces urogenitalis</i> DSM 15434	Low M _m polyPase I	Actinobacteria	
B3DSU9	<i>Bifidobacterium longum</i> DJO10A	Low M _m polyPase I	Actinobacteria	
K0HUJ5	<i>Propionibacterium acnes</i> C1	Low M _m polyPase I	Actinobacteria	
F5XTP2	<i>Micrococcus phosphovorans</i> ATCC 700054	Low M _m polyPase I	Actinobacteria	
Q0RCH1	<i>Frankia alni</i> ACN14a	Low M _m polyPase I	Actinobacteria	
Q2RMA7	<i>Moorella thermoacetica</i> ATCC 39073	Low M _m polyPase I	Clostridia	
Q8NRR8	<i>Corynebacterium glutamicum</i> ATCC 13032	Low M _m polyPase I	Actinobacteria	Lindner et al. 2009
Q8NT99	<i>Corynebacterium glutamicum</i> ATCC 13032	Low M _m polyPase II	Actinobacteria	Lindner et al. 2009
P9WHV5	<i>Mycobacterium tuberculosis</i> H37Rv	Low M _m polyPase I	Actinobacteria	Choi et al. 2012
L7N5A6	<i>Mycobacterium tuberculosis</i> H37Rv	Low M _m polyPase II	Actinobacteria	Choi et al. 2012
Q9RJD5	<i>Streptomyces coelicolor</i> ATCC BAA-471	Low M _m polyPase II (D)	Actinobacteria	
Q9X8H1	<i>Streptomyces coelicolor</i> ATCC BAA-471	Low M _m polyPase II (D)	Actinobacteria	
Q5HWB4	<i>Campylobacter jejuni</i> RM1221	Low M _m polyPase II (D)	ε proteobacteria, Campylobacteriales	
Q5HTM6	<i>Campylobacter jejuni</i> RM1221	Low M _m polyPase II (D)	ε proteobacteria, Campylobacteriales	
B3DRI3	<i>Bifidobacterium longum</i> DJO10A	Low M _m polyPase II	Actinobacteria	
O67040	<i>Aquifex aeolicus</i> VF5	Low M _m polyPase II	Aquificae	Kristensen et al. (2008)
Q9WY38	<i>Thermotoga maritima</i> ATCC 43589	Low M _m polyPase II	Thermotogae	
B7H8Y4	<i>Bacillus cereus</i> B4264	Low M _m polyPase II	Bacilli	
D5AWL8	<i>Rickettsia prowazekii</i> Rp22	Low M _m polyPase II	α proteobacteria, Rickettsiales	
Q9ZMF7	<i>Helicobacter pylori</i> ATCC 700824	Low M _m polyPase II	ε proteobacteria, Campylobacteriales	
Q9A7L4	<i>Caulobacter crescentus</i> ATCC 19089	Large polyPase	α proteobacteria, Caulobacteriales	
Q9A7V5	<i>Caulobacter crescentus</i> ATCC 19089	Low M _m polyPase I	α proteobacteria, Caulobacteriales	
D5APK2	<i>Rhodobacter capsulatus</i> ATCC BAA-309	Large polyPase	α proteobacteria, Rhodobacteriales	
D5ATS3	<i>Rhodobacter capsulatus</i> ATCC BAA-309	Low M _m polyPase I	α proteobacteria, Rhodobacteriales	
G2TD63	<i>Rhodospirillum rubrum</i> F11	Large polyPase	α proteobacteria, Rhodospirillales	Albi T. and Serrano A., unpublished
G2T6W5	<i>Rhodospirillum rubrum</i> F11	Low M _m polyPase I	α proteobacteria, Rhodospirillales	Albi T. and Serrano A.,

				unpublished
F1YSZ5	<i>Acetobacter pomorum</i> DM001	Large polyPase	α proteobacteria, Rhodospirillales	
F1YW03	<i>Acetobacter pomorum</i> DM001	Low M_m polyPase I	α proteobacteria, Rhodospirillales	
F6ET83	<i>Sphingobium chlorophenicum</i> L-1	Large polyPase	α proteobacteria, Sphingomonadales	
F6ETM8	<i>Sphingobium chlorophenicum</i> L-1	Low M_m polyPase I	α proteobacteria, Sphingomonadales	
Q2IX62	<i>Rhodopseudomonas palustris</i> HaA2	Large polyPase	α proteobacteria, Rhizobiales	
Q2IV67	<i>Rhodopseudomonas palustris</i> HaA2	Low M_m polyPase I	α proteobacteria, Rhizobiales	
Q983V2	<i>Rhizobium loti</i> MAFF303099	Large polyPase	α proteobacteria, Rhizobiales	
Q983F9	<i>Rhizobium loti</i> MAFF303099	Low M_m polyPase I	α proteobacteria, Rhizobiales	
F6E5H9	<i>Sinorhizobium meliloti</i> AK83	Large polyPase	α proteobacteria, Rhizobiales	
F6E0Q3	<i>Sinorhizobium meliloti</i> AK83	Low M_m polyPase I	α proteobacteria, Rhizobiales	
Q1MIW5	<i>Rhizobium leguminosarum</i> bv. <i>viciae</i> 3841	Large polyPase	α proteobacteria, Rhizobiales	
Q1ML16	<i>Rhizobium leguminosarum</i> bv. <i>viciae</i> 3841	Low M_m polyPase I	α proteobacteria, Rhizobiales	
C4IQ36	<i>Brucella abortus</i> 2308 A	Large polyPase	α proteobacteria, Rhizobiales	
C4IVF6	<i>Brucella abortus</i> 2308 A	Low M_m polyPase I	α proteobacteria, Rhizobiales	
F2K6P2	<i>Pseudomonas brassicacearum</i> NFM421	PolyPase, GPPase- like (D)	γ proteobacteria, Enterobacteriales	
F2KFQ6	<i>Pseudomonas brassicacearum</i> NFM421	PolyPase, GPPase- like (D)	γ proteobacteria, Enterobacteriales	
P0AFL6	<i>Escherichia coli</i> K12	PolyPase, GPPase- like	γ proteobacteria, Enterobacteriales	Akiyama et al. 1993
P25552	<i>Escherichia coli</i> K12	GPPase	γ proteobacteria, Enterobacteriales	Keasling et al. 1993
P0A269	<i>Salmonella typhimurium</i> ATCC 700720	PolyPase, GPPase- like	γ proteobacteria, Enterobacteriales	
P0A267	<i>Salmonella typhimurium</i> ATCC 700720	GPPase	γ proteobacteria, Enterobacteriales	
A4TMO2	<i>Yersinia pestis</i> Pestoides F	PolyPase, GPPase- like	γ proteobacteria, Enterobacteriales	
A4TRC9	<i>Yersinia pestis</i> Pestoides F	GPPase	γ proteobacteria, Enterobacteriales	
A5F8V4	<i>Vibrio cholerae</i> serotype O1 ATCC 39541	PolyPase, GPPase- like	γ proteobacteria, Vibrionales	
A5F3R3	<i>Vibrio cholerae</i> serotype O1 ATCC 39541	GPPase	γ proteobacteria, Vibrionales	
B5XNP3	<i>Klebsiella pneumoniae</i> 342	PolyPase, GPPase- like	γ proteobacteria, Enterobacteriales	
B5XYZ0	<i>Klebsiella pneumoniae</i> 342	GPPase	γ proteobacteria, Enterobacteriales	
Q5GWJ8	<i>Xanthomonas oryzae</i> pv. <i>oryzae</i> KACC10331	PolyPase, GPPase- like	γ proteobacteria, Xanthomonadales	
PPX HAEIN P44828 E2MQ81	<i>Haemophilus influenzae</i> ATCC 51907	PolyPase, GPPase- like	γ proteobacteria, Pasteurellales	
	<i>Francisella novicida</i> FTG	PolyPase, GPPase- like	γ proteobacteria, Thiotrichales	

B5S2R3	<i>Ralstonia solanacearum</i> MolK2	PolyPase, GPPase-like	β proteobacteria, Burkholderiales
Q12BB8	<i>Polaromonas</i> sp. ATCC BAA-500	PolyPase, GPPase-like	β proteobacteria, Burkholderiales
Q9JYR3	<i>Neisseria meningitidis</i> serogroup B (MC58)	PolyPase, GPPase-like	β proteobacteria, Neisseriales
Q6MA81	<i>Protochlamydia amoebophila</i> UWE25	RTG2 cluster	Chlamydiae
C9RK29	<i>Fibrobacter succinogenes</i> ATCC 19169	RTG2 cluster (D)	Fibrobacteres
D9S6A7	<i>Fibrobacter succinogenes</i> ATCC 19169	RTG2 cluster (D)	Fibrobacteres
D0KUG5	<i>Sulfolobus solfataricus</i> 98/2	Low M _m polyPase II	A, Crenarchaeota
F8ANL1	<i>Methanothermococcus okinawensis</i> DSM 14208	Low M _m polyPase II	A, Euryarchaeota
Q46D77	<i>Methanosarcina barkeri</i> (strain Fusaro / DSM 804)	PolyPase-HD	A, Euryarchaeota
D4AUM1	<i>Arthroderma benhamiae</i> ATCC MYA-4681	RTG2 protein	E, Fungi
G4MSF6	<i>Magnaporthe oryzae</i> ATCC MYA-4617	RTG2 protein	E, Fungi
C4R4L3	<i>Pichia pastoris</i> ATCC 20864	RTG2 protein	E, Fungi
C5PH82	<i>Coccidioides posadasii</i> C735	RTG2 protein	E, Fungi
J3KIN4	<i>Coccidioides immitis</i> RS	RTG2 protein	E, Fungi
Q6CR66	<i>Kluyveromyces lactis</i> ATCC 8585	RTG2 protein	E, Fungi
C8Z806	<i>Saccharomyces cerevisiae</i> (Baker's yeast)	RTG2 protein	E, Fungi
F2SKX6	<i>Trichophyton rubrum</i> ATCC MYA-4607	RTG2 protein	E, Fungi
A9V304	<i>Monosiga brevicollis</i>	RTG2 cluster	E, Choanoflagellida
F2UAY9	<i>Salpingoeca</i> sp. ATCC 50818	RTG2 cluster	E, Choanoflagellida

Most of the Ppx-GppA proteins listed are putative, and are selected based on the Ppx-GppA domain assignment recorded in the UniProtKG database.

(**D**), pairs of close paralogs located in the same cluster of sequences. **E**, Eukaryotes; **A**, Archaea.

Low M_m polyPase I, sequences of the Low M_m polyPases-NTPases assembly in the phylogenetic tree of Fig. 5; Low M_m polyPase II, sequences of the Low M_m polyPases (II) cluster in Fig. 5; PolyPase-HD, sequences of the HD-domain polyPases assembly in Fig. 5; Large polyPase, sequences of the High-M_m polyPases cluster in Fig. 5.